Localization of both SOD1 and SOD2 in the cochlea has been reported [7], and SOD1 is the most abundant in the cochlea, comprising approximately 74% of total SOD activity [8]. Absence of SOD1 has been shown to lead to an increase in hearing loss related to acoustic trauma [9]. In addition, auditory dysfunction due to noise exposure is attenuated by application of SOD1 [10]. Furthermore, transgenic mice overexpressing SOD1 were protected against aminoglycoside-induced hearing loss, which is also mediated by ROS [11]. However, no protective effects of overexpression of SOD1 against acoustic trauma were observed [12]. Therefore, the protective effects of SOD1 against acoustic trauma remain unresolved.

SOD1 has been suggested as a possible therapeutic tool for treating ROS-related diseases. However, its rapid metabolic clearance and low affinity to cell membrane limit its clinical application. Lecithinized SOD1 (PC-SOD1), which is produced by binding lecithin (phosphatidylcholine) derivatives to each SOD1 dimer [13], has a high affinity to the cell membrane and shows a delayed plasma disappearance. In this study, we examined the effects of acoustic trauma in mice receiving lecithinized PC-SOD1 [13] as well as in transgenic mice overexpressing SOD1, and discuss the complexity of oxidative metabolism in the cochlea.

Materials and methods

The experimental protocols evaluation of the effects of PC-SOD1 were approved by the *Animal Research Committee*, Graduate School of Medicine, Kyoto University. Animal care was under the supervision of the Institute of Laboratory Animals, Graduate School of Medicine, Kyoto University. Experiments on transgenic mice were carried out at the University of Michigan. Studies at the University of Michigan were in compliance with guidelines of the National Institutes of Health and the Declaration of Helsinki and were approved by the University of Michigan's Committee on Use and Care of Animals. Animal care was under the supervision of the University of Michigan's Unit for Laboratory Animal Medicine.

PC-SOD1 application

C57BL/6 mice at 12 weeks of age (purchased from Japan SLC Inc., Hamamatsu, Japan) were used as experimental animals. PC-SOD1 (gift Dr. Rie Igarashi, St. Marianna University, Japan) is produced by binding four molecules of the lecithin (phosphatidylcholine) derivatives to each SOD1 dimer [13]. PC-SOD1, dissolved in physiological saline, was injected intraperitoneally at a concentration of 5000 U/kg (0.2 ml, at pH 7.0) 30 min before noise exposure (PC-SOD group). Animals injected with physiological saline alone were used as controls (SAL group). The animals were exposed to 8 kHz octave band noise at 115 dB SPL for 1 h in a ventilated sound exposure chamber while having free access to food and water. The sound levels were monitored and calibrated at multiple locations within the sound chamber to ensure uniformity of the stimulus. The animals treated with PC-SOD1, but not exposed to the noise (Control group), were also examined to evaluate the effects of the application of PC-SOD1 alone on auditory function.

SOD1-overexpressed mice

Transgenic mice *(C57BL/6-TgN [SOD1] 3Cje)* carrying extra copies of human cytoplasmic Cu/Zn-SOD (h-SOD1) [14] were obtained from Dr. Charles Epstein and bred at the University of Michigan. They were maintained by backcrossing to C57BL/6. Transgenic animals at 5 weeks of age (Tg) were used as experimental animals. Age-matched wild-type animals (Wt) served as controls. The animals were exposed to broadband noise (2–20 kHz) at 110 dB SPL for 2 h in a ventilated sound exposure chamber while having free access to food and water.

Measurement of hearing

To assess auditory function, the auditory brain stem response (ABR) was measured. In PC-SOD1 experiments (PC-SOD group; $n = 10$, SAL group; $n = 10$), measurements of ABR thresholds were performed preexposure and 2 h, 3 days, or 14 days after noise exposure. Thresholds were determined for frequencies of 10, 20, and 40 kHz. ABRs of the Control group animals ($n = 4$) were measured at the same time points. Measurements of ABR in transgenic animals ($n = 6$) and their littermates ($n = 4$) followed an essentially similar protocol, and were performed preexposure and 2 h, 4 days, or 14 days after noise exposure. Thresholds were determined for frequencies of 6, 12, and 24 kHz.

Animals were anesthetized with ketamine (100 mg/kg) and xylazine (9 mg/kg) by intraperitoneal injection and kept warm with a heating pad. Generation of acoustic stimuli and subsequent recording of evoked potentials were performed using a PowerLab/4 sp (AD Instruments, Castle Hill, Australia). Acoustic stimuli, consisting of tone burst stimuli (0.1 ms $\cos^2$ rise/fall and 1 ms plateau), were delivered monaurally through a speaker (ES1spc, Bioresearch Center Nagoya, Japan) connected to a funnel fitted into the external auditory meatus. To record bioelectrical potentials, subdermal stainless-steel needle electrodes were inserted at the vertex (ground), ventrolateral to the measured ear (active) and contralateral to the measured ear (reference). Stimuli were calibrated against a 1/4-inch free-field microphone (ACO-7016, ACO Pacific, Inc., Belmont, CA) connected to an oscilloscope (DS-8812 DS-538, Iwatsu Electric, Tokyo, Japan) or a sound level meter (LA-5111, Ono Sokki, Yokohama, Japan). The responses between the vertex and mastoid subcutaneous electrodes were amplified with a

digital amplifier (MA2, Tucker-Davis Technologies, Alachua, FL). Thresholds were determined from a set of responses at varying intensities with 5 dB SPL intervals and electrical signals were averaged for 512 or 1024 repetitions. Thresholds at each frequency were verified at least twice.

An overall effect on threshold shifts of the application of PC-SOD1 or SOD1 transgene was examined by the two-way factorial ANOVA. A P value less than 0.05 was considered statistically significant. When the interaction was significant, multiple comparisons with the Tukey-Kramer test were used for pairwise comparisons.

Measurement of SOD activity

The SOD activity in the cochlea was assessed by a SOD assay kit-WST (Dojindo Molecular Technologies, Inc., Gaithersburg, MD). Cochlear specimens were obtained from animals of the PC-SOD (n = 5) or physiologic saline group (n = 5) 2 h after exposure to 8 kHz octave band noise at 115 dB SPL for 1 h. Each cochlea homogenate (whole-cell extract) was prepared by freeze-grinding the dissected 2 cochleae from each animal (approximately 50 mg in weight) in 20 mM phosphate buffer, pH 7.4. The homogenate was subjected to low-speed centrifugation at 3000 g for 15 min at 4°C. An aliquot of 20 μl supernatant was applied in each well of a 96-well plate and added with 200 μl of WST Working Solution and then mixed. After the addition of 20 μl of Enzyme Working Solution, each sample was incubated at 37°C for 20 min, and then the absorbance at 450 nm was detected using a microplate reader (FLUOstar Optima, BMG Lab Technologies Inc., Durham, NC). The SOD activity (U/mg) in the PC-SOD group was compared with that in the SAL group by the unpaired t test. A P value less than 0.05 was considered statistically significant.

Measurement of catalase activity

Hydrogen peroxide generated by a reaction of superoxide and SOD is partly catalyzed by catalase. We measured the activity for catalase in cochlear specimens after noise exposure with or without application of PC-SOD to determine the influence of increasing SOD1 on the activity of these enzymes. The catalase activity in the cochlea was assessed by a catalase assay kit (Cayman Chemical Company, Ann Arbor, MI). Cochlear specimens were obtained from animals of the PC-SOD (n = 10) or physiologic saline group (n = 10) 2 h after the noise exposure. Each cochlea homogenate (whole-cell extract) was prepared by the method described above. An aliquot of 20 μl supernatant was applied in each well of 96-well plate added with 100 μl of assay buffer and 30 μl of methanol. The reaction was initiated by adding 20 μl of hydrogen peroxide and incubated for 20 min at room temperature on a shaker. Potassium hydroxide was added to terminate the reaction, and then each sample was incubated with 30 μl of Purpald (chromogen) for 10 min at room temperature. After the addition of 10 μl of potassium periodate, each sample was incubated for 5 min, and then the absorbance at 540 nm was detected using a microplate reader (FLUOstar Optima, BMG Lab Technologies Inc.). The catalase activity (nmol/min/ml) in the PC-SOD group was compared with that in the SAL group by the unpaired t test. A P value less than 0.05 was considered statistically significant.

Results

Supplementation with PC-SOD1

In the Control group, no significant alteration in ABR thresholds was observed (Fig. 1A), indicating that applica-

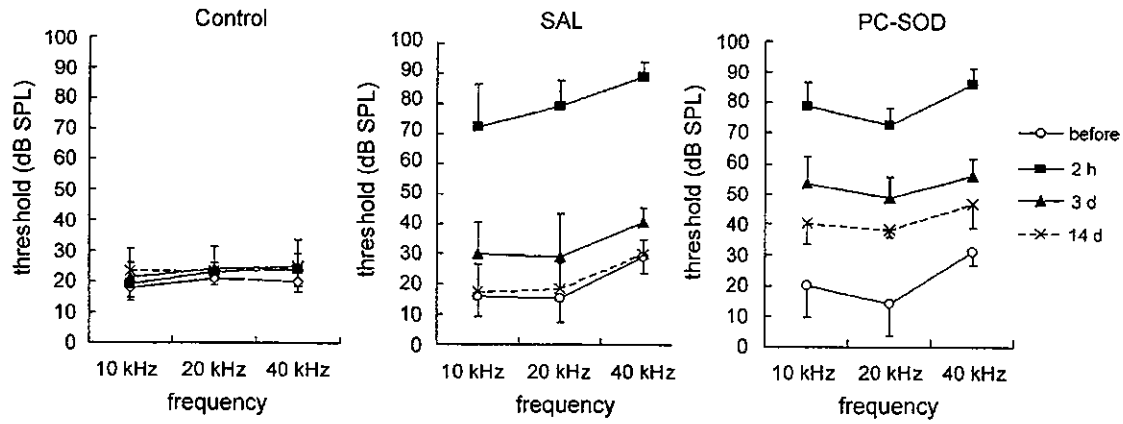

Fig. 1. Time courses of alteration in ABR thresholds of C57BL/6 mice treated with lecithinized copper/zinc-superoxide dismutase and not exposed to noise (Control group; A), those treated with lecithinized copper/zinc-superoxide dismutase and exposed to noise (PC-SOD group; B), or those treated with physiological saline and exposed to noise (SAL group; C). The y axis depicts ABR thresholds in dB SPL and the x axis shows the tested frequencies.The Control group demonstrates no alteration in ABR thresholds (A). The PC-SOD group exhibits severe elevation of thresholds 2 h after noise exposure and a trend to decrease thresholds (B). ABR thresholds of the SAL group also elevate 2 h after noise exposure, and return to almost preexposure levels 14 days after exposure (C). Error bars represent standard deviations.

tion of PC-SOD1 has no effects on auditory function without noise exposure. In the SAL group, ABR thresholds were elevated between 56 dB SPL at 10 kHz and 63 dB SPL at 20 kHz 2 h after noise exposure (Fig. 1C). Elevation of thresholds was still observed 3 days after noise exposure, although thresholds tended to recover. However, ABR thresholds recorded 14 days after exposure had nearly returned to preexposure values. Identically with the SAL group, the SOD group also exhibited threshold shifts between 55 dB SPL at 40 kHz and 58.6 dB SPL at 20 kHz 2 h after exposure (Fig. 1B). However, recovery of ABR thresholds 3 days after noise exposure was less than that found in the SAL group. In contrast to the SAL group, ABR thresholds in the PC-SOD group exhibited poor recovery 14 days after exposure.

The time course of alterations in ABR threshold shifts following noise exposure at 10 or 20 kHz is shown in Fig. 2. The following discussion emphasizes results at 10 and 20 kHz. Tests at 40 kHz gave similar results. An overall

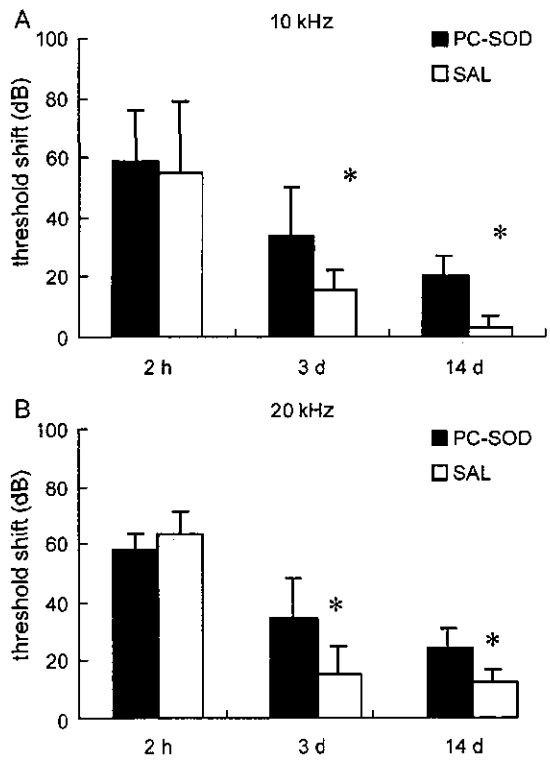

Fig. 2. ABR threshold shifts following noise exposure at 10 and 20 kHz in animals treated with lecithinized copper/zinc-superoxide dismutase (PC-SOD) or physiological saline (SAL). The y axis depicts ABR threshold shifts in dB and the x axis shows the time points of measurements following noise exposure. The difference in threshold shifts between the PC-SOD and SAL group at 10 kHz is significant at $P = 0.003$ (A), and that at 20 kHz (B) is significant at $P = 0.0009$ for the two-way factorial ANOVA. Differences in threshold shifts at 10 kHz between two groups 3 and 14 days after noise exposure are significant (asterisks in A), and those at 20 kHz are significant in multiple comparisons with the Tukey-Kramer test (asterisks in B). Error bars represent standard deviations.

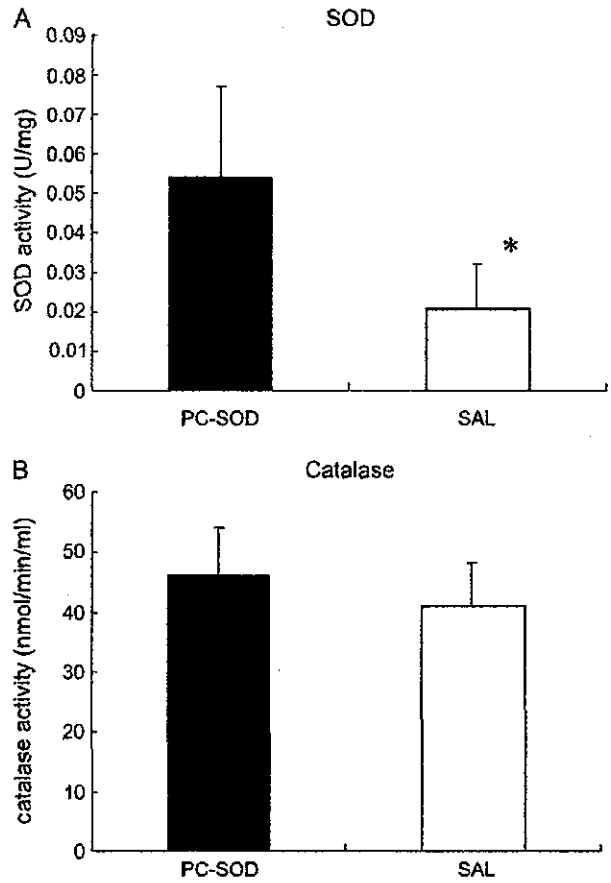

Fig. 3. SOD and catalase activity in cochlear extracts from animals treated with lecithinized copper/zinc-superoxide dismutase (PC-SOD) or physiological saline (SAL) 2 h after noise exposure. The SOD1 activity (A) of the PC-SOD group is significantly higher than that of the SAL group (asterisk: unpaired t test, $P < 0.05$), while no significant difference in the catalase activity (B) is found. Error bars represent standard deviations.

effect on data for 10 kHz of PC-SOD1 application was significant ($P = 0.003$). The differences in threshold shifts between PC-SOD 3 days and SAL 3 days and between PC-SOD 14 days and SAL 14 days were significant in multiple comparisons with the Tukey-Kramer method. An overall effect on data for 20 kHz of PC-SOD1 application was significant ($P = 0.0009$). Multiple comparisons with the Tukey-Kramer method demonstrated significant differences in threshold shifts between PC-SOD 3 days and SAL 3 days and between PC-SOD 14 days and SAL 14 days.

The SOD activity of cochleae extract was 0.054 and 0.023 U/mg (mean and standard deviation) in the PC-SOD group, and 0.021 and 0.009 in the SAL group. The difference in the SOD activity between the two groups was statistically significant (Fig. 3A). In contrast to the findings in the SOD activity, no significant difference in the catalase activity of cochleae was found between the two groups (Fig. 3B). The catalase activity of cochleae extract was 46.09 and 8.02 nmol/min/ml (mean and standard

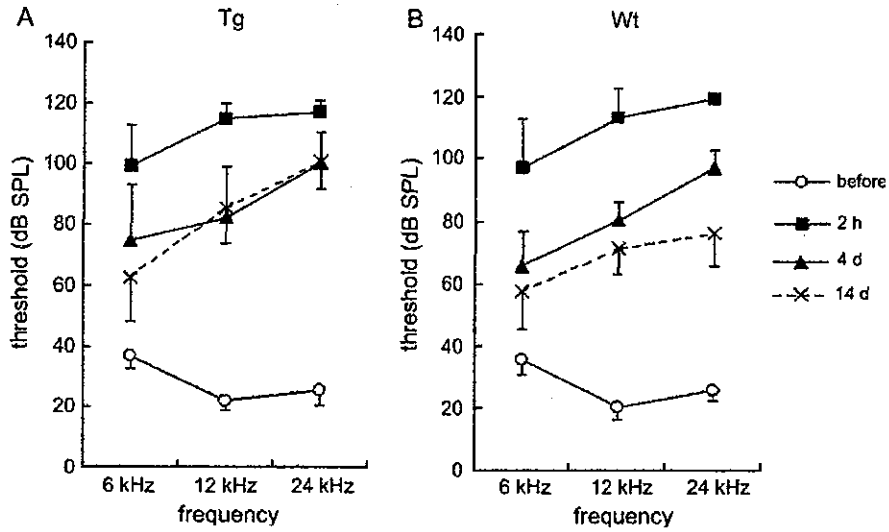

Fig. 4. Time courses of alteration in auditory brainstem response (ABR) thresholds of transgenic mice overexpressing human copper/zinc-superoxide dismutase (Tg; A) or wild-type animals (Wt; B) following noise exposure. The *y* axis depicts ABR thresholds in dB SPL and the *x* axis shows the tested frequencies. Exposure to broadband noise (2–20 kHz) at 110 dB SPL for 2 h causes threshold shifts in both transgenic (A) and wild-type animals (B). A decrease in ABR thresholds of wild-type mice is observed between 4 and 14 days after noise exposure, while no recovery is found in ABR thresholds at 12 and 24 kHz of transgenic mice. Error bars represent standard deviations.

deviation) in the PC-SOD group, and 41.04 and 4.73 in the SAL group.

Transgenic mice overexpressing SOD

Exposure to broadband noise (2–20 kHz) at 110 dB SPL for 2 h caused elevation of ABR thresholds in both Tg and Wt animals (Fig. 4). Two hours after noise exposure, threshold shifts were identical in the two groups of animals. ABR thresholds of Tg animals decreased 4 days after noise exposure as well as those of Wt animals. However, no recovery in ABR thresholds at 12 and 24 kHz was found in Tg animals 14 days after noise exposure, while Wt animals exhibited further recovery.

The time course of alterations in ABR threshold shifts at 12 or 24 kHz following noise exposure is shown in Fig. 5. Threshold shifts were identical in the two groups of animals 2 h and 4 days after noise exposure. After 14 days, however, threshold shifts in Tg animals remained as high as 4 days, while those in Wt animals tended to decrease. However, an overall effect on data for 12 kHz of the SOD1 transgene was not significant ($P = 0.27$). On the other hand, an overall effect on data for 24 kHz of the SOD1 transgene was significant ($P = 0.034$). A difference between Wt 14 days and Tg 14 days was significant in multiple comparisons with the Tukey-Kramer method.

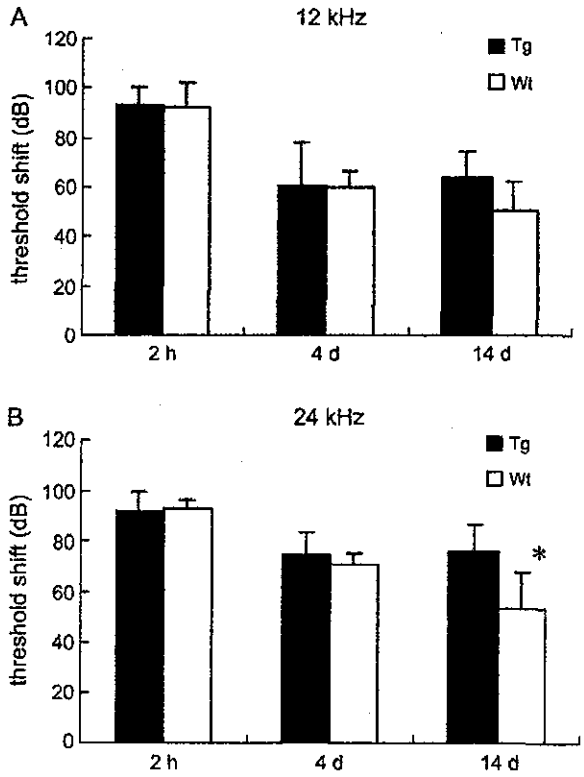

Fig. 5. ABR threshold shifts following noise exposure at 12 and 24 kHz in transgenic (Tg) and wild-type (Wt) mice. The *y* axis depicts ABR threshold shifts in dB and the *x* axis shows the time points of measurements following noise exposure. The difference in threshold shifts between the Tg and the Wt group at 12 kHz (A) is not significant ($P = 0.27$), but that at 24 kHz (B) is significant for the two-way factorial ANOVA ($P = 0.034$). The difference in threshold shifts at 24 kHz between two groups 14 days after noise exposure is significant in multiple comparisons with the Tukey-Kramer test (asterisk in B). *Error* bars represent standard deviations.

Discussion

Antioxidants and enzymes associated with cellular antioxidant defenses are expected to provide protection against pathologies that are based on the formation of ROS.

There is ample evidence in this regard, including studies in the auditory system showing attenuation of drug-induced (cisplatin and aminoglycosides), noise-induced, and ischemic hearing loss by a variety of antioxidants [3,4,15,16]. Increasing the activity of superoxide dismutase, the enzyme that-in conjunction with catalase and glutathione peroxidase (GPx)-inactivates superoxide should therefore also be an effective protectant. This is indeed the case in aminoglycoside-induced hearing loss [6]. In noise-induced hearing loss (NIHL), which is also based on the formation of superoxide and other ROS [2,3,17,18], this protection is not consistently effective [10,20].

In fact, it is most likely that the high levels of SOD reverse the expected protective action and actually have a detrimental influence. This "SOD paradox" is a well-documented phenomenon. Toxicity of high concentrations of SOD has been reported in a variety of systems [14,19–21]. However, the pathways to mediate toxicity of excessive SOD have not been elucidated. Removal of superoxide depends on SOD; the removal of hydrogen peroxide depends on catalase and GPx. Therefore, efficient scavenging of superoxide requires not only an elevated SOD but also an elevated level of catalase or GPx. An imbalance in the activity of these enzymes therefore results in an accumulation of hydrogen peroxide. Hydrogen peroxide itself is highly toxic, and can then cause cellular damage via the formation of hydroxyl radicals in a Fenton reaction. This pathway is a candidate implicating toxicity of excessive SOD to cochleae. In the present study, SOD increased in the cochlea without a concomitant increase of catalase. These findings support this hypothesis. However, other pathways implicating the toxicity of excessive SOD have been proposed [22]. Therefore, further studies are needed to determine the actual mechanisms for toxicity of excessive SOD to cochleae.

McFadden et al. [23] reviewed the influence of SOD1 deficiency on NIHL. A series of their experiments in which subject ages and conditions of noises are relevant variables has revealed that SOD1 deficiency has little influence on the magnitude of PTS. In addition, young SOD1-deficient mice exhibit less susceptibility to NIHL than age-matched wild-type animals. Based on these findings, they have proposed the hypothesis that SOD1 deficiency causes a decrease of hydroxyl radicals, resulting in relative protection from noise trauma. The data presented by Coling et al. [12] show higher, but not statistically significant, threshold shifts in SOD1 transgenic animals than wild-type animals. The present findings demonstrate that elevating SOD1 levels enhance NIHL. These data for effects of SOD1 deficiency and excessive SOD1 on NIHL indicate a close relation between changes in the levels of SOD1 and those of hydroxyl radicals in cochleae.

The trend toward a higher NIHL in SOD-overexpressing and PC-SOD-treated animals to noise exposure is similar, although less pronounced in the transgenic mice. This quantitative difference may arise from the fact that the time course for increasing SOD activity is quite different between PC-SOD1 and transgenic mice. In PC-SOD1 animals, an increase of SOD1 in the cochlea rapidly occurs and declines, while expression of SOD1 in transgenic animals is constitutively elevated. It is therefore possible that overexpression of SOD1 results in concomitant changes in the levels of other antioxidant enzymes while the rapid alteration in the levels of SOD1 in PC-SOD1 animals may not cause such changes. In fact, no significant differences in the levels of catalase were found between PC-SOD1- and saline-treated animals in the present study.

The rapid degradation of exogenous SOD1 is an important issue for systemic administration of exogenous SOD1. Derivatives with longer half-lives are generally more successful. PC-SOD1, designed to target cell membranes, has higher tissue accumulation as well as a longer blood half-life than unmodified SOD1 [13] and has a stronger protective effect against ROS-induced tissue injury than polyethylene glycol-SOD1 [24]. In fact, cochlear specimens of the PC-SOD group animals exhibited about 2.6-fold SOD activity of the SAL, showing that systemic application of PC-SOD1 actually results in accumulation of PC-SOD1 in the cochlear specimens. There is a discrepancy in the effects of exogenous SOD1 application between the findings in the literature [10] and the present findings. In the present findings, PC-SOD1 showed detrimental effects on NIHL in mice, while application of polyethylene glycol-SOD1 was found to attenuate NIHL in rats [10]. We consider that the discrepancy can be interpreted by the difference in time points for measurements of auditory thresholds, although the differences in animal species and exposed noise are probably included as causes for the discrepancy. Protective effects of polyethylene glycol-SOD1 were determined only by measurements of auditory thresholds immediately after noise exposure. Auditory thresholds at 20 and 40 kHz 2 h after noise exposure in saline-treated animals are also higher than those in PC-SOD1-treated animals in the present study, although the differences are not statistically significant. In addition, elevation of the levels of SOD in the cochlea was not confirmed in this previous study. Therefore, the actual effects of polyethylene glycol-SOD1 on NIHL, especially effects on PTS, are still controversial.

Our data point to the complexity of ROS homeostasis and "Antioxidant treatment" is not always effective: the noise conditions and the type of pharmacological protection will determine whether the outcome is positive or negative. Further studies are needed to more fully elucidate the mechanisms of ROS-induced stress in the cochlea and the most appropriate treatment for protection.

Acknowledgments

We thank Prof. Igarashi for providing lecithinized Cu/Zn superoxide dismutase and for helpful suggestions for this study. This study was supported by a Grant-in-Aid

for Scientific Research from the Ministry of Education, Science, Sports, Culture, and Technology of Japan, and by Grant DC-03685 from the National Institutes of Deafness and Communication Disorder, National Institutes of Health (to J.S.).

References

[1] Nordmann, A. S.; Bohne, B. A.; Harding, G. W. Histopathological differences between temporary and permanent threshold shift. *Hear Res.* **139**:13–30; 2000.

[2] Yamane, H.; Nakai, Y.; Takayama, M.; Iguchi, H.; Nakagawa, T.; Kojima, A. Appearance of free radicals in the guinea pig inner ear after noise-induced acoustic trauma. *Eur. Arch. Otorhinolaryngol.* **252**: 504–508; 1995.

[3] Ohinata, Y.; Miller, J. M.; Altschuler, R. A.; Schacht, J. Intense noise induces formation of vasoactive lipid peroxidation products in the cochlea. *Brain Res.* **878**:163–173; 2000.

[4] Ohlemiller, K. K.; Dugan, L. L. Elevation of reactive oxygen species following ischemia-reperfusion in mouse cochlea observed in vivo. *Audiol. Neurootol.* **4**:219–228; 1999.

[5] Staecker, H.; Zheng, Q. Y.; Van De Water, T. R. Oxidative stress in aging in the C57Bl6/J mouse cochlea. *Acta Otolaryngol.* **121**:666–672; 2001.

[6] Sha, S. H.; Schacht, J. Antioxidants attenuate gentamicin-induced free radical formation in vitro and ototoxicity in vivo. *Hear. Res.* **142**: 34–40; 2000.

[7] Rarey, K. E.; Yao, X. Localization of Cu/Zn-SOD and Mn-SOD in the rat cochlea. *Acta Otolaryngol.* **116**:833–835; 1996.

[8] Pierson, M. G.; Gray, B. H. Superoxide dismutase activity in the cochlea. *Hear. Res.* **6**:141–151; 1982.

[9] Ohlemiller, K. K.; McFadden, S. L.; Ding, D. L.; Flood, D. G.; Reaume, A. G.; Hoffman, E. K.; Scott, R. W.; Wright, J. S.; Putcha, G. V.; Salvi, R. J. Targeted deletion of the cytosolic Cu/Zn-superoxide dismutase gene (Sod1) increases susceptibility to noise-induced hearing loss. *Audiol. Neurootol.* **4**:237–246; 1999.

[10] Seidman, M. D.; Shivapuja, B. G.; Quirk, W. S. The protective effects of allopurinol and superoxide dismutase on noise-induced cochlear damage. *Otolaryngol. Head Neck Surg.* **109**:1052–1056; 1993.

[11] Sha, S. H.; Zajic, G.; Epstein, C. J.; Schacht, J. Overexpression of SOD protects from kanamycin-induced hearing loss. *Audiol. Neurootol.* **6**:117–123; 2001.

[12] Coling, D. E.; Yu, K. C.; Somand, D.; Satar, B.; Bai, U.; Huang, T. T.; Seidman, M. D.; Epstein, C. J.; Mhatre, A. N.; Lalwani, A. K. Effect of SOD1 overexpression on age- and noise-related hearing loss. *Free Radic. Biol. Med.* **34**:873–880; 2003.

[13] Igarashi, R.; Hoshino, J.; Takenaga, M.; Kawai, S.; Morizawa, Y.; Yasuda, A.; Otani, M.; Mizushima, Y. Lecithinization of superoxide dismutase potentiates its protective effect against Forssman antiserum-induced elevation in guinea pig airway resistance. *J. Pharmacol. Exp. Ther.* **262**:1214–1219; 1992.

[14] Epstein, C. J.; Avraham, K. B.; Lovett, M.; Smith, S.; Elroy-Stein, O.; Rotman, G.; Bry, C.; Groner, Y. Transgenic mice with increased Cu/Zn-superoxide dismutase activity: animal model of dosage effects in Down syndrome. *Proc. Natl. Acad. Sci. USA* **84**:8044–8048; 1987.

[15] Li, G.; Sha, S. H.; Zotova, E.; Arezzo, J.; Van De Water, T.; Schacht, J. Salicylate protect hearing and kidney function from cisplatin toxicity without compromising its oncolytic action. *Lab. Invest.* **82**: 585–596; 2002.

[16] Wu, W. J.; Sha, S. H.; Schacht, J. Recent advances in understanding aminoglycoside ototoxicity and its prevention. *Audiol. Neurootol.* **7**: 171–174; 2002.

[17] Rao, D. B.; Moore, D. R.; Reinke, L. A.; Fechter, L. D. Free radical generation in the cochlea during combined exposure to noise and carbon monoxide: an electrophysiological and an EPR study. *Hear. Res.* **161**:113–122; 2001.

[18] Van Campen, L. E.; Murphy, W. J.; Franks, J. R.; Mathias, P. I.; Toraason, M. A. Oxidative DNA damage is associated with intense noise exposure in the rat. *Hear. Res.* **164**:29–38; 2002.

[19] Ceballos, I.; Nicole, A.; Briand, P.; Grimber, G.; Delacourte, A.; Flament, S.; Blouin, J. L.; Thevenin, M.; Kamoun, P.; Sinet, P. M. Expression of human Cu-Zn superoxide dismutase gene in transgenic mice: model for gene dosage effect in Down syndrome. *Free Radic. Res. Commun.* **12–13**:581–589; 1991.

[20] Fullerton, H. J.; Ditelberg, J. S.; Chen, S. F.; Sarco, D. P.; Chan, P. H.; Epstein, C. J.; Ferriero, D. M. Copper/zinc superoxide dismutase transgenic brain accumulates hydrogen peroxide after perinatal hypoxia ischemia. *Ann. Neurol.* **44**:357–364; 1998.

[21] De Haan, J. B.; Newman, J. D.; Kola, I. Cu/Zn superoxide dismutase mRNA and enzyme activity, and susceptibility to lipid peroxidation, increases with aging in murine brains. *Mol. Brain Res.* **13**:179–186; 1992.

[22] Kowald, A.; Klipp, E. Alternative pathways might mediate toxicity of high concentrations of superoxide dismutase. *Ann. N.Y. Acad. Sci.* **1019**:370–374; 2004.

[23] McFadden, S. L.; Ding, D.; Ohlemiller, K. K.; Salvi, R. J. The role of superoxide dismutase in age-related and noise-induced hearing loss: clues from SOD1 knockout mice. In: Willott, J. F., ed. *Handbook of mouse auditory research from behavior to molecular biology.* Boca Raton: CRC Press; 2001:489–504.

[24] Igarashi, R.; Hoshino, J.; Ochiai, A.; Morizawa, Y.; Mizushima, Y. Lecithinized superoxide dismutase enhances its pharmacologic potency by increasing its cell membrane affinity. *J. Pharmacol. Exp. Ther.* **271**:1672–1677; 1994.

Original Paper

Audiology & Neuro-Otology

Audiol Neurootol 2005;10:97–104
DOI: 10.1159/000083365

Received: February 19, 2004
Accepted after revision: August 11, 2004
Published online: January 12, 2005

Aging Effects on Vestibulo-Ocular Responses in C57BL/6 Mice: Comparison with Alteration in Auditory Function

Atsushi Shiga[a] Takayuki Nakagawa[b] Meiho Nakayama[a] Tsuyoshi Endo[b]
Fukuichiro Iguchi[b] Tae-Soo Kim[b] Yasushi Naito[b] Juichi Ito[b]

[a]Department of Otolaryngology, Aichi Medical University, Aichi, and [b]Department of Otolaryngology Head and Neck Surgery, Kyoto University Graduate School of Medicine, Kyoto, Japan

Key Words
Aging · Auditory brainstem response · Cochlea · Ampullar crista · Vestibulo-ocular reflex

Abstract
Age-related changes in auditory function are well documented in animal models; however, this is not the case as regards vestibular function. In this study, we evaluated age-related changes in vestibulo-ocular responses in C57BL/6 mice that are considered as a model of presbycusis. The functional data were substantiated by the findings of histological analysis of vestibular and auditory peripherals. The gain in vestibulo-ocular reflex, which reflects functionality of the vestibular system, increased in an age-dependent manner until 12 weeks and exhibited limited functional loss due to aging after 24 weeks. By contrast, no alteration in the thresholds of the auditory brainstem response (ABR) was observed from 3 to 12 weeks of age; however, ABR thresholds were significantly elevated from age 24 weeks and onwards. Histological analysis demonstrated that the degeneration of auditory peripherals was closely related with functional loss due to aging. Vestibular peripherals also exhibited age-related degeneration morphologically, although age-related dysfunction was not apparent. Age-related changes in the vestibular function of C57BL/6 mice followed a different time course when compared to changes in auditory function. These findings indicate that mechanisms for age-related changes in vestibular function differ from those of auditory function.

Introduction

Hearing, balance and gait disturbance is frequently observed in older people, and such symptoms are often the cause of disability in daily life. Considering the current increase in the aged population, it is important to seek methods to overcome age-related auditory and vestibular dysfunction. The mechanisms involved in age-related changes in auditory and vestibular function have been investigated using animal and human subjects. Animal models have been reported for the study of age-related changes in hearing [Hequembourg and Liberman, 2001; Bartolome et al., 2002; Henry, 2002], especially aging-induced sensorineural hearing loss (presbycusis). In contrast to auditory function, an animal model for the study of age-related vestibular dysfunction has not been established, although age-related changes in vestibular function have been investigated in humans [Peterka et al.,

KARGER
Fax + 41 61 306 12 34
E-Mail karger@karger.ch
www.karger.com

1420–3030/05/0102–0097$22.00/0

Accessible online at:
www.karger.com/aud

Takayuki Nakagawa, MD, PhD
Department of Otolaryngology-Head and Neck Surgery
Graduate School of Medicine, Kyoto University
Kawaharacho 54, Shogoin, Sakyo-ku, 606-8507 Kyoto (Japan)
Tel. +81 75 751 3346, Fax +81 75 751 7225, E-Mail tnakagawa@ent.kuhp.kyoto-u.ac.jp

1990; Paige 1992; Enrietto et al., 1999; Baloh et al., 2003]. Therefore, little is known about the mechanisms involved in age-related changes as regards vestibular function.

Aging is associated with degeneration of the auditory and vestibular peripherals in animals [Park et al., 1987; Keithley et al., 1989; Nakayama et al., 1994; Gratton MA and Schulte BA, 1995; Spongr et al., 1997; Hequembourg and Liberman, 2001] and humans [Schuknecht, 1974; Lopez et al., 1997]. However, the relationship between age-related degeneration in the peripheral sensory organs and functional loss has been controversial, especially in relation to vestibular systems. It is certain that age-related changes in the central systems also contribute to auditory and vestibular dysfunction [Enrietto et al., 1999].

The C57BL/6 mouse has long been considered, in scores of published studies, to be a model of early adult-onset, progressive sensorineural hearing loss [Spongr et al., 1997; Hequenbourg and Liberman, 2001; McFadden et al., 2001; Bartolome et al., 2002; Henry, 2002]. Age-related changes in the auditory systems of C57BL/6 mice have been well documented in terms of function and morphology. However, the details of age-related changes in the vestibular function of C57BL/6 mice have not been elucidated. In this study, we observed horizontal vestibulo-ocular reflex (VOR) responses of C57BL/6 mice during aging and compared VORs with auditory brainstem responses (ABRs) measured over the same time course. In parallel to functional assessments, morphological changes in the auditory and vestibular peripherals were examined to elucidate the relationship between age-related degeneration in the peripheral sensory organs and functional loss. In auditory peripherals, we focused on degeneration of the auditory sensory epithelium, the organ of Corti, auditory primary neurons, and spiral ganglion neurons (SGNs). In vestibular peripherals, degeneration of ampullar cristae of the lateral semicircular canals (LSCCs) was evaluated, because signals from the LSCC are crucial for the horizontal VOR.

Materials and Methods

Experimental Animals

C57BL/6 mice (Japan SLC Inc., Hamamatsu, Japan) aged 3 (n = 5), 6 (n = 5), 12 (n = 5), 24 (n = 5) and 60 weeks (n = 4) were used as experimental animals and divided into 5 experimental groups according to their ages. The animals had free access to water and a normal mouse diet (MF, Oriental Yeast, Chiba, Japan). All experimental protocols were approved by the Animal Research Committee, Graduate School of Medicine, Kyoto University. Animal care was under the supervision of the Institute of Laboratory Animals, Graduate School of Medicine, Kyoto University.

Measurement of Vestibulo-Ocular Responses

The horizontal VOR responses were recorded using an infrared video oculogram system [Funabiki et al., 1999]. The left eye was used for monitoring. An aluminum platform was glued on to the cranial bone using dental cement under general anesthesia with ketamine (100 mg/kg) and xylazine (9 mg/kg). The animal was mounted on a turntable by attachment of the aluminum platform, and the body of the animal was supported with a rubber sheet. The head of the animal was tilted 35° nose down so that the LSCCs were positioned approximately parallel to the horizontal plane. Sinusoidal oscillations of 1.8–115° (center to peak) at 0.1–3.2 Hz were applied to the turntable at the maximum angular head velocity, i.e. 30 degrees/s. The animals were sinusoidally oscillated at 0.4, 0.8 or 1.6 Hz in the dark in order to evoke horizontal eye responses. Horizontal eye position was stored as an ASCII file and then analyzed to compute the gain and phase of the VOR responses [Iwashita et al., 2001].

Measurement of ABRs

ABR measurements were performed under general anesthesia with ketamine (100 mg/kg) and xylazine (9 mg/kg). Animals were placed inside a sound isolated booth. Generation of acoustic stimuli and subsequent recording of evoked potentials were performed using a PowerLab/4sp (AD Instruments, Castle Hill, Australia). Acoustic stimuli, consisting of tone burst stimuli (0.1 ms $\cos^2$ rise/fall and 1 ms plateau), were delivered monaurally through a speaker (ES1spc, Bioresearch Center, Nagoya, Japan), connected to a funnel, fitted into the external auditory meatus. To record bioelectrical potentials, subdermal stainless steel needle electrodes were inserted at the vertex (ground), ventrolateral to the measured ear (active) and contralateral to the measured ear (reference). Stimuli were calibrated against a 1/4-inch free-field mike (ACO-7016, ACO Pacific Inc., Belmont, Calif., USA) connected to an oscilloscope (DS-8812 DS-538, Iwatsu Electric, Tokyo, Japan) or a sound level meter (LA-5111, Ono Sokki, Yokohama, Japan). Responses between the vertex and mastoid subcutaneous electrodes were amplified with a digital amplifier (MA2, Tucker-Davis Technologies, Alachua, Fla., USA). Thresholds were determined for frequencies of 4, 8, 16 and 32 kHz from a set of responses at varying intensities with 5-dB SPL intervals, and electrical signals were averaged at 512 repetitions. In case of scale-out, thresholds were defined as the maximum intensity of the tone burst stimuli plus 5 dB SPL for statistical analysis.

Histological Analysis

After functional analysis, the animals were deeply anesthetized with a lethal dose of ketamine and xylazine and were perfused intracardially with physiological saline, followed by 4% paraformaldehyde in 0.01 *M* phosphate-buffered saline (PBS) at pH 7.4. Excised temporal bones were immersed in the same fixative at 4°C for 4 h. The ampullar cristae of the LSCCs and cochleae were dissected from the temporal bones in PBS. Cochlear specimens were then placed into 0.1 *M* ethylenediaminetetraacetic acid in PBS for decalcification. The samples were incubated with 30% sucrose in PBS at 4°C prior to embedding in OCT compound (Tissue-Tek, Sakura Finetechnical, Tokyo, Japan) and frozen at −80°C. The entire length of the crista (transverse to the flow of endolymph) was sectioned into 10-μm slices. Mid-modiolus sections of cochleae were prepared for histological analysis.

We evaluated age-related histological changes in the cristae and cochleae using hematoxylin-eosin (HE) staining and immunohistochemistry. In the ampullar cristae of the LSCCs, the density of hair

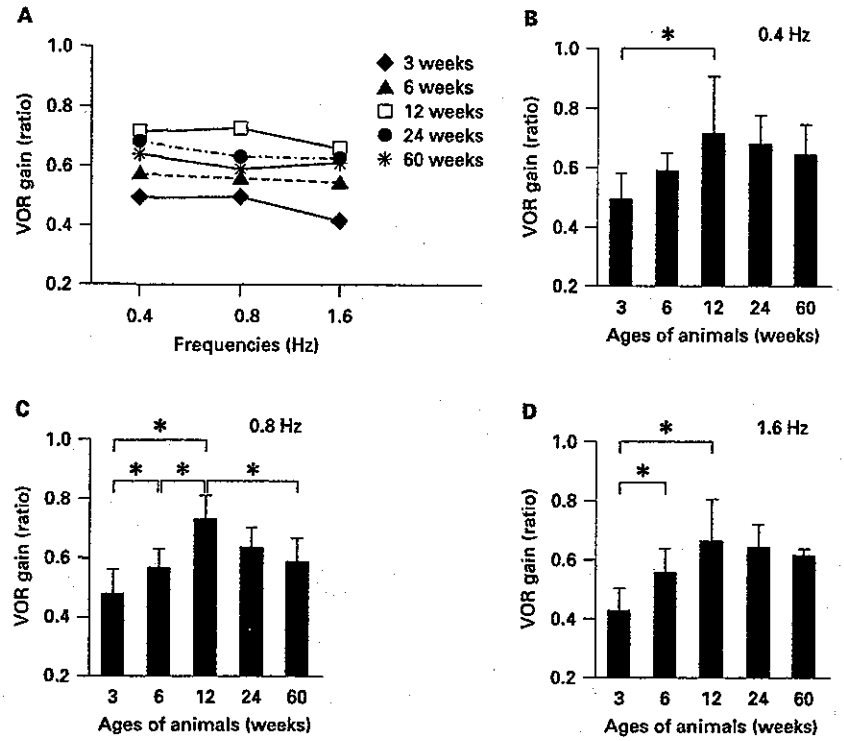

Fig. 1. Effect of aging on VOR gains. **A** The means of VOR gains at 0.4, 0.8 or 1.6 Hz sinusoidal oscillation are represented. VOR gains increase during 3–12 weeks of age, and gradually decrease after 12 weeks of age. The means and standard deviations at 0.4 Hz (**B**), 0.8 Hz (**C**) and 1.6 Hz (**D**) are represented for all ages evaluated. Asterisks show the statistical significant differences at $p < 0.05$ (ANOVA with Scheffé's method for significance).

cells was evaluated using immunohistochemistry for myosin VIIa. Four out of every 20 sections of cristae were provided for immunohistochemical analysis. Anti-myosin VIIa rabbit polyclonal antibody (a gift from Tama Hasson, University of California San Diego, San Diego, Calif., USA) diluted 1:200 in PBS was used as the primary antibody, and Alexa-488 conjugated anti-rabbit goat IgG (Molecular Probes, Eugene, Oreg., USA) diluted 1:500 in PBS was used as the secondary antibody, followed by counterstaining with 4′,6-diamino-2-phenylindole dihydrochloride (DAPI; 2 μg/ml PBS, Molecular Probes). Myosin VIIa and DAPI double-positive cells were identified as hair cells. The length of the basement membrane of sensory epithelia was measured with the use of NIH image software. The hair cell density was determined as the number of hair cells per 1 mm of the basement membrane in each specimen. The average of the hair cell densities from 4 sections of cristae was defined as the data for the animal.

Degeneration of inner hair cells (IHCs) and outer hair cells (OHCs) in the organ of Corti, and SGNs were morphologically evaluated using mid-modiolus sections stained with HE. In addition, we quantitatively assessed the density of SGNs by the use of immunostaining for class III β-tubulin (TuJ1). The density of SGNs was calculated in every turn of cochleae from 4 sections of each animal. Anti-TuJ1 mouse monoclonal antibody (Covance Research Product, Berkeley, Calif., USA) diluted 1:200 in PBS was used as the primary antibody, and Alexa-594 conjugated anti-mouse goat IgG (Molecular Probes) diluted 1:200 in PBS was used as the secondary antibody. Counterstaining with DAPI was performed to demonstrate nuclear chromatin. SGNs were identified by the combined presence of TuJ1 and DAPI. The area of the Rosenthal's canal was measured with the use of NIH image software. The SGN density of each turn of cochleae was determined as the number of SGNs per 1 mm^2 of the Rosenthal's canals. The average of the numbers of SGN densities from 4 sections of cochleae was defined as the data for the animal.

Statistical Analysis

Data were statistically evaluated by analysis of variance using the Scheffé's method for the determination of significance ($p < 0.05$). StatView software (StatView version 5.0, SAS Institute Inc., Cary, N.C., USA) was used.

Results

Effects of Aging on Vestibulo-Ocular Responses

Animals at 3 weeks of age exhibited the lowest gain of VOR at every frequency among all experimental groups (fig. 1A). The gains of VOR then increased in an age-dependent manner until the experimental animals reached 12 weeks of age (fig. 1B–D). The differences in the gains of VOR between 3 and 12 weeks of age at every frequency, and between 3 and 6 weeks of age at 1.6 Hz were statistically significant. The increase in gains tended to be large at high frequencies. Gains of VOR peaked at

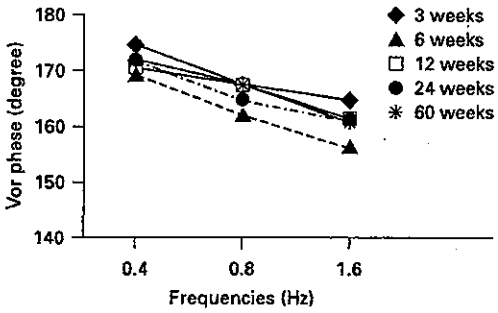

2

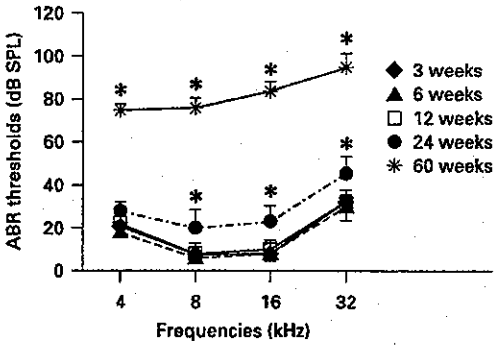

3

Fig. 2. Effect of aging on VOR phases. The means of VOR phases at 0.4, 0.8 or 1.6 Hz sinusoidal oscillation are represented for all ages evaluated. No significant differences in VOR phases among experimental groups are found.

Fig. 3. Effects of aging on ABR thresholds. The means and standard deviations of ABR thresholds at all stimulation frequencies are represented for all ages evaluated. Significant elevation in thresholds are observed at 24 weeks of age at 8, 16 and 32 kHz, and at 60 weeks of age at all stimulation frequencies. * $p < 0.05$ by ANOVA with Scheffé's method for significance.

12 weeks of age, and no differences in gains among evaluated frequencies were observed. These findings suggest that the VOR is still developing during the young-adult period of life in C57BL/6 mice. By contrast, the phases of VOR showed no significant alteration during this period (fig. 2).

The VOR gains exhibited a trend to decrease in an age-dependant manner in animals above 12 weeks of age; however, its decrease was limited (fig. 1). A significant difference in the gains of VOR was only found between mice of 12 and 60 weeks of age at 0.8 Hz (fig. 1C). In comparison with the age-related increase observed in young-adult animals, the age-related decrease in the gains of VOR was small. These findings indicate that VOR responses are maintained at least until 60 weeks of age in C57BL/6 mice. By contrast, no significant differences in the phases of VOR among experimental groups were observed during this period (fig. 2). The phases of VOR exhibited almost no alteration from 3 to 60 weeks of age in C57BL/6 mice.

Effects of Aging on ABRs

In contrast to VOR responses, ABR thresholds exhibited no age-related alteration at any frequencies from 3 to 12 weeks of age (fig. 3). The mean values obtained from animals at 3, 6 and 12 weeks of age were almost identical, and no significant differences in ABR thresholds were found among them.

Above 12 weeks of age, severe hearing loss due to aging was demonstrated by ABR measurements (fig. 3). At 24 weeks of age, ABR thresholds were moderately elevated at every frequency in comparison to those measured at 12 weeks of age. Threshold shifts at 24 weeks of age compared to ABR thresholds measured at 12 weeks of age ranged from 6.2 dB SPL at 4 kHz to 13.6 dB SPL at 32 kHz. Differences in ABR thresholds at 8, 16 and 32 kHz between mice of 12 and 24 weeks of age were statistically significant (fig. 3). A severe elevation of ABR thresholds was observed at 60 weeks of age. ABR thresholds at 16 and 32 kHz were scaled out in most experimental animals at 60 weeks of age. Threshold shifts at 60 weeks of age compared to ABR thresholds measured at 12 weeks of age ranged from 53.0 dB SPL at 4 kHz to 72.9 dB SPL at 16 kHz. Differences in ABR thresholds between mice at 60 weeks of age and other experimental groups were statistically significant at every frequency (fig. 3).

Morphological Changes in Ampullar Cristae

The ampullar cristae of the LSCCs obtained from animals at 3, 6 and 12 weeks of age exhibited no degenerative changes in sensory epithelia. Immunostaining for myosin VIIa clearly demonstrated the localization of hair cells (fig. 4A, B). The densities of hair cells at 3, 6 and 12 weeks of age were approximately 100 cells/mm (fig. 4C). No significant differences were found among them. In the vestibular epithelia of animals at 24 weeks of age, mild degeneration was observed. Partial loss of hair cells was observed, mainly in the apex of ampullar cristae. The density of hair cells at 24 weeks of age decreased to about 80% of that present at 3 weeks of age (fig. 4C). Differences in the densities of hair cells between 24 and 3, 6 or 12 weeks of age were statistically significant. At 60 weeks of age, loss of hair cells in the apex of ampullar cristae was more

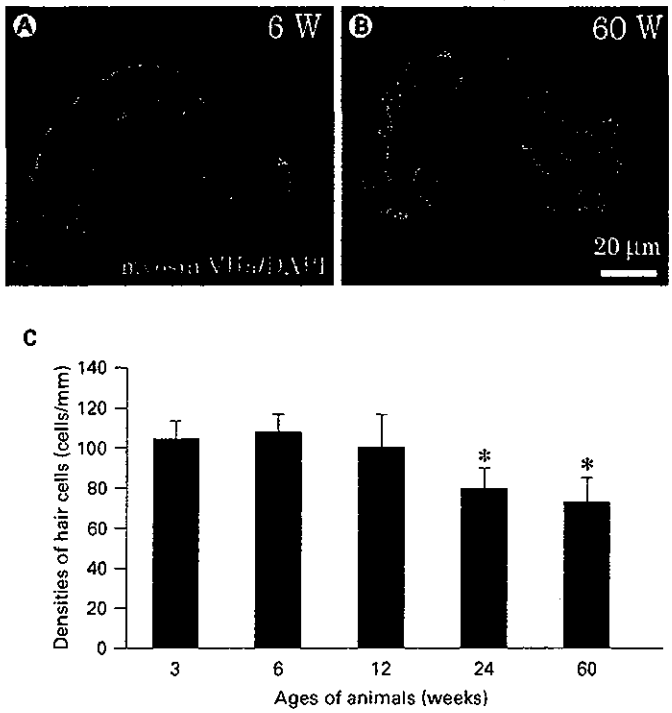

Fig. 4. Effects of aging on the densities of vestibular hair cells in lateral semicircular canals. Vestibular hair cells in ampullar cristae are clearly labeled by immunohistochemistry for myosin VIIa (green), and their nuclei are stained with DAPI (blue). No degenerative changes in the sensory epithelium are observed at 6 weeks of age (**A**), while loss of hair cells is found in the apex of the crista at 60 weeks of age (**B**). Scale bar represents 30 μm. The means and standard deviations of densities of hair cells are represented for all ages evaluated (**C**). A significant decrease in densities is found at 24 and 60 weeks of age. * $p < 0.05$ by ANOVA with Scheffé's method for significance.

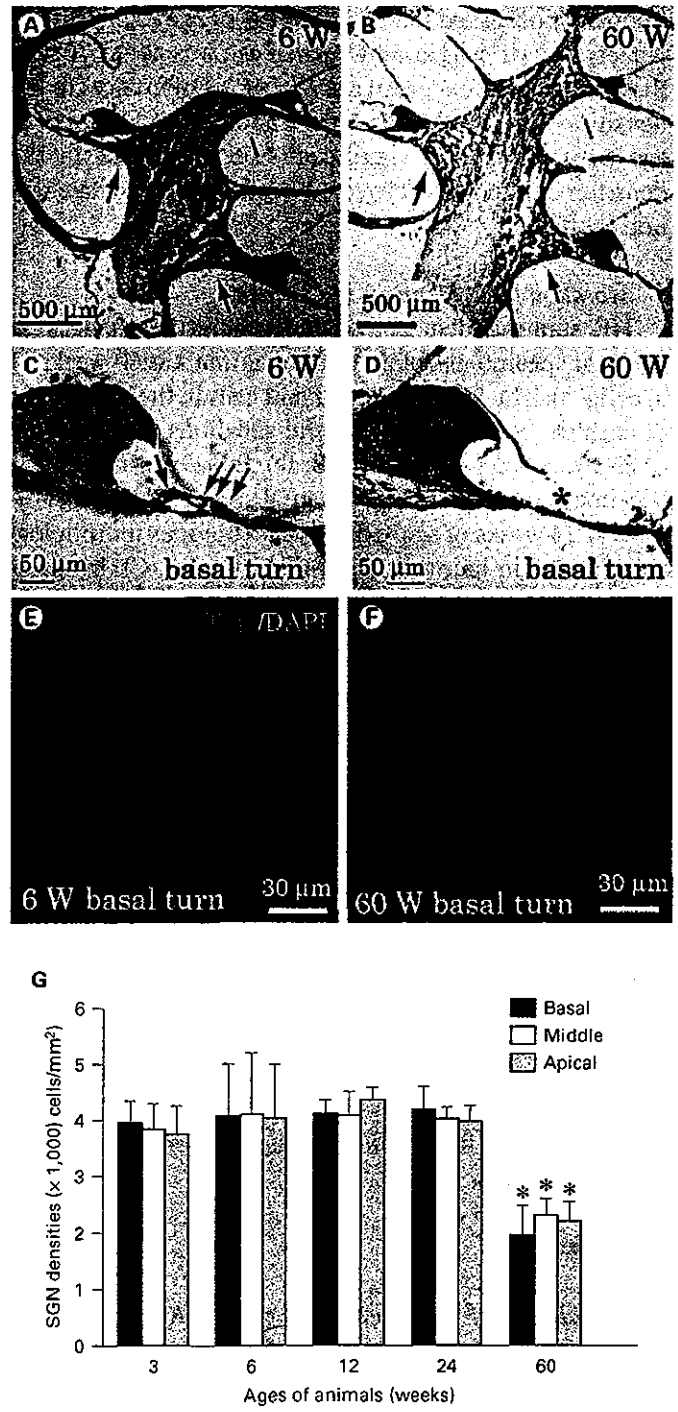

Fig. 5. Effects of aging on cochlear morphology. Mid-modiolus sections of cochleae at 6 (**A**) and 60 weeks of age (**B**) stained with HE. Arrows represent the location of spiral ganglions. Scale bar represents 500 μm. Atrophic changes in spiral ganglions are remarkable in a section at 60 weeks of age. HE staining demonstrates 3 OHCs (red arrows) and a single IHC (black arrow) in the basal turn of the cochlea at 6 weeks of age (**C**). In contrast, total loss of hair cells (asterisk) is identified in the basal turn of the cochlea at 60 weeks of age (**D**). Scale bars represent 50 μm. SGNs are labeled by immunohistochemistry for TuJ1 (red). DAPI staining (blue) shows the location of nuclei. The number of SGNs at 60 weeks of age (**F**) appears to be lower than that at 6 weeks of age (**E**). Scale bar represents 30 μm. The means and standard deviations of SGN densities in every cochlear turn are represented for all ages evaluated (**G**). A significant decrease in densities is found at 60 weeks of age in every cochlear turn. * $p < 0.05$ by ANOVA with Scheffé's method for significance.

frequently observed than at 24 weeks of age (fig. 4B). The density of hair cells at 60 weeks of age was about 70% of that recorded at 3 weeks of age (fig. 4C). Differences in the densities of hair cells between 60 and 3, 6 or 12 weeks of age were statistically significant. The difference in the densities of hair cells between 24 and 60 weeks of age was not significant.

Morphological Changes in Cochleae

HE staining demonstrated degenerative changes in cochlear specimens obtained from animals at 60 weeks of age (fig. 5). The loss of cochlear hair cells in the basal turns of cochleae and atrophy of spiral ganglions in every turn of cochleae were noted (fig. 5B, D). By contrast, cochlear specimens from other experimental groups, including animals at 24 weeks of age, exhibited no obvious morphological changes in hair cells and SGNs (fig. 5A, C). In specimens at 60 weeks of age, the loss of OHCs was frequently observed in the basal turns of cochleae (fig. 5D), while in the other turns of cochleae, loss of OHCs was not obvious. IHC loss was observed in the basal turn (fig. 5D), but in neither the middle nor apical turns of cochleae. In short, a significant loss of hair cells and SGNs was found in cochleae at 60 weeks of age, but not in those at 24 weeks of age.

Quantitative assessment of SGN degeneration was performed using sections stained for TuJ1, a marker for neurons (fig. 5E, F). No significant alteration in SGN densities was found among mice of 3, 6, 12 and 24 weeks of age, but SGN densities at 60 weeks of age were significantly decreased in every turn of cochleae (fig. 5G). The mean of the SGN densities at 60 weeks of age was approximately 50% of that recorded at 3 weeks of age in the basal turn, and 60% of that in the middle or apical turn.

Discussion

Correlation of VOR Responses with ABRs

The C57BL/6 mouse is considered a model of early adult-onset, progressive sensorineural hearing loss. The time course of progression of hearing loss in C57BL/6 mice has been well documented [Hequenbourg and Liberman, 2001; Bartolome et al., 2002; Henry, 2002]. These previous studies have demonstrated that hearing loss in C57BL/6 mice begins at 24 weeks of age, and progresses to deafness at 60 weeks of age, which is identical to the present findings, as a result of ABR analysis. In animal experiments, the measurement of VOR responses has frequently been used to examine loss and recovery of vestibular function [Black et al., 1987; Carey et al., 1996; Goode et al., 1999; Fetoni et al., 2003]. We therefore employed measurements of VOR responses to evaluate the vestibular function of C57BL/6 mice.

C57BL/6 mice exhibited a trend towards an age-related decrease in VOR gains above 12 weeks of age; however, significant decreases in VOR gains were found only at 0.8 Hz between 12 and 60 weeks of age. At 0.4 and 1.6 Hz, there were no significant decreases in VOR gains in mice above 12 weeks of age. No severe dysfunction of VOR responses was observed at these frequencies at 24 and 60 weeks of age, while significant elevation of ABR thresholds was found in these animals. These findings demonstrate that the age-related dysfunction of auditory systems is not correlated with that of vestibular systems in C57BL/6 mice, which is identical to previous findings in a longitudinal study in humans [Enrietto et al., 1999].

Another discrepancy in age-related changes between vestibular and auditory function was found between 3 and 12 weeks of age. ABR thresholds at 3 weeks of age were the same as those at 12 weeks of age, while VOR gains at 3 weeks of age were significantly lower than those at 12 weeks of age. From 3 to 12 weeks of age, an age-dependent increase in VOR gains was observed, indicating that the vestibular function of C57BL/6 mice was still developing during this period. These findings indicate that there is a delay in the functional maturation of vestibular systems when compared with that of auditory systems in C57BL/6 mice. Such a delay in the functional maturation of vestibular systems has also been observed in the kitten. The development of VOR responses in the kitten is complete at 8 weeks of age [Flandrin et al., 1979], while ABR thresholds are generally within adult range by 3 weeks of age [Walsh et al., 1986]. By comparison, the mouse cochlea appears to be histologically mature by the end of 3 weeks of age [Lim and Rueda, 1992], indicating that functional maturation of the mouse auditory system may parallel its anatomical maturation. The anatomical maturation of the mouse peripheral vestibular system is almost complete by 23 days after birth [Desmadryl et al., 1992]. Thus, the present findings demonstrate that functional maturation of the mouse vestibular function is delayed in relation to its anatomical maturation. Postnatal developmental changes in VOR responses have been reported in the rat and guinea pig, and these cannot be due to the increasing size of semicircular canals [Curthoys, 1979; Curthoys et al., 1982]. Therefore, functional maturation of the mouse vestibular system may reflect the development of central vestibular networks. More studies on the developmental changes in both the central and

peripheral vestibular systems are necessary to elucidate the mechanisms involved in the delay of maturation in vestibular function.

Correlation of Functional Loss with Morphological Degeneration

In the present study, the degeneration of cochlear hair cells and SGNs appeared to occur in parallel with a progression in hearing loss, which is identical to previous findings. The loss of OHCs was predominantly observed in the basal turns of cochleae, and the loss of IHCs was limited in the basal turns. However, a significant elevation of ABR thresholds appeared at both low and high frequencies. Therefore, the functional loss cannot occur by the morphological degeneration of cochlear hair cells alone, although this factor does contribute to auditory dysfunction. By contrast, a decrease in SGN densities was found from the basal to the apical parts of cochleae. Some previous studies support the hypothesis that SGN loss is the predominant cause of age-related hearing loss [Keithley et al., 1989; Slepecky et al., 2000].

In the present study, morphological degeneration was also found in the vestibular epithelia of aged animals. Hair cell density decreased by 20–30% in the ampullar cristae of the LSCCs in aged animals, which is identical to previous findings [Park et al., 1987]. Hair cell deletion was predominantly observed in the apex of cristae in aged animals similar to previous findings in human subjects [Rosenhall, 1973]. However, VOR responses of aged animals were well maintained even at 60 weeks of age. These findings indicate that age-related dysfunction of vestibular sensory epithelia does not correlate well with the morphological degeneration of vestibular peripherals. Enrietto et al. [1999] indicated that age-related changes in vestibular function likely result from those in the central nervous system rather than those in peripheral structures. Age-related degeneration of vestibular nuclei has also been demonstrated morphologically [Lopez et al., 1997]. On the other hand, the head velocity of rotation can be a cause for the discrepancy between histological and functional findings in vestibular systems in the present study. In human subjects, no age-associated decrease in VOR gains is observed when sinusoidal oscillations are applied at the head velocity ranging from 20 to 60 degrees/s [Wall et al., 1984], while the use of sinusoidal oscillations applied at the head velocity ranging from 50 to 300 degrees/s has caused a decrease in VOR gain in the elderly [Paige, 1992]. Therefore, the head velocity can affect findings on age-related changes in VOR gain. In the present study, we did not examine the effects of head velocities on alteration in age-related changes in VOR gains of C57BL/6 mice. The effects of head velocity on VOR gains in aged C57BL/6 mice must therefore be examined in the near future. In addition, the effects of vestibular compensation, the plasticity of the vestibular system [Precht, 1986; Curthoys, 2000], could contribute to the maintenance of VOR responses in aged animals. A significant process of compensation follows in the weeks or months after the damage of vestibular peripherals. However, vestibular compensation in relation to age-related changes in the vestibular system has not yet been elucidated.

Several animal experiments, however, have demonstrated that the loss of vestibular hair cells is well correlated with a decrease in VOR gains [Black et al., 1987; Carey et al., 1996; Fetoni et al., 2003]. Acute degeneration of vestibular epithelia in these experiments was induced by ototoxic treatments. In addition, the majority of hair cells were disrupted by ototoxic treatments. In contrast to ototoxic treatment models, 70% of hair cells remained in the vestibular epithelia of aged animals in our study, and the deletion of hair cells occurred more slowly. These differences in the process of hair cell degeneration between ototoxic treatments and aging could cause differences in alteration in VOR gains.

Conclusions

The present findings demonstrate the different time sequences of age-related changes in vestibular and auditory function in C57BL/6 mice and the contribution of peripheral degeneration to functional alteration. In auditory systems, changes in the peripheral system are closely related with functional maturation and age-related dysfunction. In contrast to the auditory system, age-associated degeneration of the peripheral vestibular system has no significant correlation with age-associated changes in vestibular function. These findings indicate that mechanisms for age-related changes in vestibular function differ from those of auditory function.

Acknowledgements

This study was supported by a grant-in-aid for scientific research, a grant-in-aid for exploratory research and a grant-in-aid for the regenerative medicine realization project from the Ministry of Education, Science, Sports, Culture and Technology of Japan. We thank Tama Hasson for providing anti-myosin VIIa antibody, and Ken Kojima, Tomoko Kita, Kazuo Funabiki and Edwin Rubel for valuable discussion and helpful comments on the manuscript.

References

Baloh RW, Ying SH, Jacobson KM: A longitudinal study of gait and balance dysfunction in normal older people. Arch Neurol 2003;60:835–839.

Bartolome MV, del CE, Lopez LM, Carricondo F, Poch-Broto J, Gil-Loyzaga P: Effects of aging on C57BL/6J mice: An electrophysiological and morphological study. Adv Otorhinolaryngol 2002;59:106–111.

Black FO, Peterka RJ, Elardo SM: Vestibular reflex changes following aminoglycoside induced ototoxicity. Laryngoscope 1987;97:582–586.

Carey JP, Fuchs AF, Rubel EW: Hair cell regeneration and recovery of the vestibuloocular reflex in the avian vestibular system. J Neurophysiol 1996;76:3301–3312.

Curthoys IS: The development of function of horizontal semicircular canal primary neurons in the rat. Brain Res 1979;167:41–52.

Curthoys IS: Vestibular compensation and substitution. Curr Opin Neurol 2000;13:27–30.

Curthoys IS, Blanks RH, Markham CH: Semicircular canal structure during postnatal development in cat and guinea pig. Ann Otol Rhinol Laryngol 1982;91:185–192.

Desmadryl G, Dechesne CJ, Raymond J: Recent aspects of development of the vestibular sense organs and their innervation; in Romand R (ed): Development of Auditory and Vestibular Systems 2. Amsterdam, Elsevier, 1992, pp 461–488.

Enrietto JA, Jacobson KM, Baloh RW: Aging effects on auditory and vestibular responses: A longitudinal study. Am J Otolaryngol 1999;20:371–378.

Fetoni AR, Sergi B, Scarano E, Paludetti G, Ferraresi A, Troiani D: Protective effects of alpha-tocopherol against gentamicin-induced Oto-vestibulo toxicity: An experimental study. Acta Otolaryngol 2003;123:192–197.

Flandrin JM, Courjon JH, Jeannerod M: Development of vestibulo-ocular response in the kitten. Neurosci Lett 1979;12:295–299.

Funabiki K, Naito Y, Matsuda K, Honjo I: A new vestibulo-ocular reflex recording system designed for routine vestibular clinical use. Acta Otolaryngol 1999;119:413–419.

Goode CT, Maney DL, Rubel EW, Fuchs AF: Visual influences on the development and recovery of the vestibuloocular reflex in the chicken. J Neurophysiol 2001;85:1119–1128.

Gratton MA, Schulte BA: Alterations in microvasculature are associated with atrophy of the stria vascularis in quiet-aged gerbils. Hear Res 1995;82:44–52.

Henry KR: Sex- and age-related elevation of cochlear nerve envelope response (CNER) and auditory brainstem response (ABR) thresholds in C57BL/6 mice. Hear Res 2002;170:107–115.

Hequembourg S, Liberman MC: Spiral ligament pathology: A major aspect of age-related cochlear degeneration in C57BL/6 mice. J Assoc Res Otolaryngol 2001;2:118–129.

Iwashita M, Kanai R, Funabiki K, Matsuda K, Hirano T: Dynamic properties, interactions and adaptive modifications of vestibulo-ocular reflex and optokinetic response in mice. Neurosci Res 2001;39:299–311.

Keithley EM, Ryan AF, Woolf NK: Spiral ganglion cell density in young and old gerbils. Hear Res 1989;38:125–133.

Lim DJ, Rueda J: Structural development of the cochlea; in Romand R (ed): Development of Auditory and Vestibular Systems 2. Amsterdam, Elsevier, 1992, pp 33–58.

Lopez I, Honrubia V, Baloh RW: Aging and the human vestibular nucleus. J Vestib Res 1997;7:77–85.

McFadden SL, Ding D, Salvi R: Anatomical, metabolic and genetic aspects of age-related hearing loss in mice. Audiology 2001;40:313–321.

Nakayama M, Helfert RH, Konrad HR, Caspary DM: Scanning electron microscopic evaluation of age-related changes in the rat vestibular epithelium. Otolaryngol Head Neck Surg 1994;111:799–806.

Paige GD: Senescence of human visual-vestibular interactions. 1. Vestibulo-ocular reflex and adaptive plasticity with aging. J Vestib Res 1992;2:133–151.

Park JC, Hubel SB, Woods AD: Morphometric analysis and fine structure of the vestibular epithelium of aged C57BL/6NNia mice. Hear Res 1987;28:87–96.

Peterka RJ, Black FO, Schoenhoff MB: Age-related changes in human vestibulo-ocular reflex: Sinusoidal rotation and caloric tests. J Vestib Res 1990;1:49–59.

Precht W: Recovery of some vestibuloocular and vestibulospinal functions following unilateral labyrinthectomy. Prog Brain Res 1986;64:381–389.

Rosenhall U: Degenerative patterns in the aging human vestibular neuro-epithelia. Acta Otolaryngol 1973;76:1973.

Schuknecht HF: Pathology of the Ear. Cambridge, Harvard UP, 1974.

Slepecky NB, Galsky MD, Swartzentruber-Martin H, Savage J: Study of afferent nerve terminals and fibers in the gerbil cochlea: Distribution by size. Hear Res 2000;144:124–134.

Spongr VP, Flood DG, Frisina RD, Salvi RJ: Quantitative measures of hair cell loss in CBA and C57BL/6 mice throughout their life spans. J Acoust Soc Am 1997;101:3546–3553.

Wall C 3rd, Black FO, Hunt AE: Effects of age, sex and stimulus parameters upon vestibulo-ocular responses to sinusoidal rotation. Acta Otolaryngol 1984;98:270–278.

Walsh EJ, McGee J, Javel E: Development of auditory-evoked potentials in the cat. 1. Onset of response and development of sensitivity. J Acoust Soc Am 1986;79:712–724.

Nuclear translocation of β-catenin in developing auditory epithelia of mice

Shinji Takebayashi,[1] Takayuki Nakagawa,[1,CA] Ken Kojima,[1,2] Tae-Soo Kim,[1] Tsuyoshi Endo,[1] Fukuichiro Iguchi,[1] Tomoko Kita,[1,3] Norio Yamamoto[4] and Juichi Ito[1]

[1]Department of Otolaryngology, Head and Neck Surgery; [2]Establishment of International COE for Integration of TransplantationTherapy and Regenerative Medicine; [3]Horizontal Medical Research Organization; [4]Department of Medical Chemistry, Kyoto University Graduate School of Medicine, Kyoto 606-8507, Japan

[CA]Corresponding Author: tnakagawa@ent.kuhp.kyoto-u.ac.jp

Received 11 January 2005; accepted 24 January 2005

β-catenin, a protein component of adherens junctions, plays a role in the signalling pathway for cell proliferation. In this study, we examined the cellular distribution of β-catenin in developing auditory epithelia of mice. Immunohistochemistry for Ki67 and cyclin D indicated active cell proliferation in premature auditory epithelia. In this period, the nuclear localization of β-catenin in epithelial cells was observed together with expression of the lymphoid enhancer factor, a transcription factor in β-catenin signalling. Epithelial cells showing nuclear localization of β-catenin disappeared at the same time, as there was a decrease of cell proliferation. These findings indicate that nuclear translocation of β-catenin plays a role in cell proliferation in developing auditory epithelia. *NeuroReport* 16:431–434 © 2005 Lippincott Williams & Wilkins.

Key words: Adherens molecule; Cell proliferation; Cochlea; Development; Sensory epithelium

INTRODUCTION

β-catenin is a pivotal component of both cadherin–catenin cell adhesion [1] and the Wnt signalling pathway, which control multiple developmental processes such as cell proliferation, migration, apoptosis and fate decision [2]. Recent studies have indicated crucial roles of β-catenin in the development of neural systems. Overexpression or ablation of β-catenin affects cell proliferation, migration and differentiation of neural precursor cells [3–5]. Inner ears have a simple cystic structure at the early stage of development, and develop a complicated structure, named labyrinth, at the late stage of development [6]. Such developmental processes of inner ears should require dexterous regulation of cell proliferation and migration. Beta-catenin is a known component of adherens junctions in developing and mature sensory epithelia of the mammalian inner ear [7–11]. Because of its dual role in cell adhesion and in cell signalling, β-catenin is a good candidate to play a central role in the control of inner ear development. However, the actual role of β-catenin in the morphogenesis of the mammalian inner ear has not been determined.

Conventional Wnt signalling increases the cytoplasmic pool of β-catenin, which translocates into the nucleus and forms a complex with the transcription factor T cell factor (TCF)/lymphoid enhancer factor (LEF) that regulates expression of important genes including cyclin D [12]. A variety of growth factor/receptor pathways also increase the cytoplasmic pool of signalling β-catenin, either by disrupting the cadherin–catenin complex or by repressing cadherin expression [13]. Thus, the key factor of β-catenin signalling is its accumulation in the cytoplasm and translocation into the nucleus.

The aim of the present study was to determine whether β-catenin plays a role in the morphogenesis of mammalian auditory epithelia. We examined changes in the cellular distribution of β-catenin in auditory epithelial cells during development using immunohistochemistry and Western blotting.

MATERIALS AND METHODS

Experimental animals: On embryonic day 9 (E9), E10, E14 or E17, ICR mouse embryos were harvested from time-mated pregnant females that had been deeply anesthetized with ketamine and xylazine. The pregnant females were then killed by cervical dislocation. The pups themselves were anesthetized via anesthesia of the mother. The Animal Research Committee, Graduate School of Medicine, Kyoto University approved all experimental protocols. Animal care was under the supervision of the Institute of Laboratory Animals, Graduate School of Medicine, Kyoto University. All experimental procedures were performed in accordance with the NIH guide for the care and use of laboratory animals.

Immunohistochemistry: Whole embryos (at E9, E10 and E14) and dissected heads (at E17) were fixed in 4% paraformaldehyde in phosphate-buffered saline (PBS; pH 7.4) at 4°C overnight (n=5 each). The samples were then cryoprotected in 30% sucrose in PBS and incubated at 4°C

for 8 h, prior to embedding in OCT compound (Tissue-Tek, Sakura Finetechnical, Tokyo, Japan), and frozen at −80°C until use. Whole heads were mounted so that sections could be cut along the dorso-ventral or anterior–posterior axis. The 10-μm-thick cryostat sections were then mounted on glass slides.

Cryostat sections were made permeable in 0.2% Triton X-100 in PBS for 30 min at room temperature. To reduce nonspecific binding, the sections were incubated in 5% skimmed milk in PBS for 15 min at room temperature. The primary antibodies used were anti-β-catenin mouse monoclonal antibody (1:100, Zymed Laboratories, South San Francisco, California, USA), anti-LEF1 mouse monoclonal antibody (1:50, Chemicon International, Temecula, California, USA), anti-cyclin D rabbit polyclonal antibody (1:100, Lab Vision Corporation, Fremont, California, USA) and anti-Ki67 rabbit polyclonal antibody (1:100, Lab Vision Corporation). The secondary antibodies were FITC-conjugated anti-mouse antibody (1:200, Chemicon International), Alexa-594-conjugated anti-rabbit antibody (1:200, Molecular Probes, Eugene, Oregon, USA) and horseradish peroxidase (HRP)-conjugated anti-mouse antibody (1:1000, Cell Signaling Technology, Beverly, Massachusetts, USA). Specimens were incubated with the primary antibodies overnight at 4°C. After PBS rinses, sections were incubated for 1 h at room temperature with the corresponding secondary antibodies. The sections with HRP-conjugated antibodies were stained with a DAB Substrate Kit for peroxidase (Vector Laboratories, Burlingame, California, USA). Nuclei were counterstained with TOTO3 (1:5000, Molecular Probes) or Meyer-hematoxylin. The samples stained with fluorescence-conjugated secondary antibodies were viewed with a Leica TCS SP2 confocal microscope (Leica Microsystems, Tokyo, Japan) and those stained with DAB were viewed with a Nikon ECLIPSE E600 microscope (Nikon, Tokyo, Japan). Specimens stained without primary antibodies were used as negative controls. Paraffin-embedded sections of human breast carcinoma (MS-1763-PCS; Lab Vision Corporation) were used as positive controls for primary antibodies.

Western blot analysis: The otic vesicles were extracted from E10 embryonic mice (n=30). Extract otocysts were suspended in the hypotonic buffer (CelLytic Nuclear Extraction Kit, Sigma-Aldrich, St Louis, Missouri, USA) and gently homogenized under the microscope. The disrupted cells were centrifuged for 20 min at 10 000g and the cytoplasmic fraction was obtained as a supernatant. After all the supernatant was fully discarded, the rest of the nuclei pellet was resuspended in extraction buffer (CelLytic Nuclear Extraction Kit). The solution was shaken gently for 30 min, centrifuged for 5 min at 20 000g, and the nuclear fraction was obtained as a supernatant. Proteins were detected using primary antibodies specific for β-catenin (1:1000, Zymed Laboratories). Nuclear and cytoplasmic fractions were monitored with anti-Ki67 antibody (1:500, Lab Vision Corporation) and anti-phosphatidylinositol 3-kinase (PI3-kinase) antibody (1:500, BD Biosciences, San Jose, California, USA), respectively. The primary antibody binding was detected with a biotinylated anti-rabbit antibody or anti-mouse antibody conjugated to alkaline phosphatase. A biotinylated secondary antibody was visualized by the avidin–biotin complex method. After PBS washes, the blots were developed with 40 mM nitro blue tetrazolium (Sigma-Aldrich) and 40 mM 5-bromo-4-chloro-3-indolyl phosphate (Sigma-Aldrich) in PBS.

RESULTS

On E9 or E10, most epithelial cell nuclei in the otic vesicle exhibited expression of Ki67 (Fig. 1b) or cyclin D (Fig. 2a), indicating active cell proliferation in developing epithelia. At this stage, intense expression of β-catenin was observed in developing epithelia. Immunolabelling for β-catenin was found not only at the plasma membrane but also in the nucleus and cytoplasm of epithelial cells (Fig. 1a–c,e–g), indicating accumulation of β-catenin in the cytoplasm of epithelial cells and its translocation into the nucleus. We performed Western blot analyses to confirm the nuclear translocation of β-catenin in otic epithelial cells on E10 (Fig. 1d). Nuclear extracts exhibited expression of Ki67, while cytoplasmic extracts exhibited expression of PI3-kinase. Both cytoplasmic and nuclear extracts demonstrated expression of β-catenin, indicating that the nuclear translocation of β-catenin occurred in otic epithelial cells on E10. In addition, the expression of LEF1 was identified in epithelial cell nuclei at this stage (Fig. 2b), indicating formation of β-catenin–LEF complexes in auditory epithelial cells.

On E14, a few cyclin D-positive cells were identified in premature auditory epithelia (Fig. 2c). The majority of epithelial cells exhibited expression of β-catenin in the location corresponding to the plasma membrane. On E17, we rarely found the cells expressing cyclin D (Fig. 2d). Immunolabelling for β-catenin was localized to the plasma membrane.

DISCUSSION

β-catenin is a structural adaptor protein linking cadherins to the actin cytoskeleton in cell–cell adhesion of inner ear sensory epithelia [7–11]. In the matured auditory epithelium, expression of β-catenin is located in the region corresponding to the cytoplasmic membrane, not in the cytoplasm or nucleus, and cell proliferation is not observed in matured auditory epithelia of mammals [14]. β-catenin plays a role not only in structural and functional integrity but also in various signalling pathways, including Wnt signalling. Conventional Wnt signalling induces accumulation of β-catenin in the cytoplasm by inhibition of glycogen synthase kinase 3-β [2]. Accumulated β-catenin is translocated into the nucleus, where it forms a complex with the transcription factor TCF/LEF that activates messenger RNA transcription associated with cell proliferation [15,16], including formation of cyclin D [6,17]. In the present study, cells in the developing auditory epithelia of mice exhibited nuclear distribution of β-catenin on E9 and E10 together with the expression of LEF1. In this period, numerous cells in auditory epithelia are undergoing cell cycle progression and proliferation, as demonstrated by immunostaining for Ki67 and cyclin D. Together with termination of cell proliferation in auditory epithelia, the cells showing nuclear or cytoplasmic distribution of β-catenin disappeared from auditory epithelia. These findings indicate that β-catenin signalling is involved in cell proliferation in auditory epithelia in the early developmental period, which is identical to previous findings in antisense experiments [9].

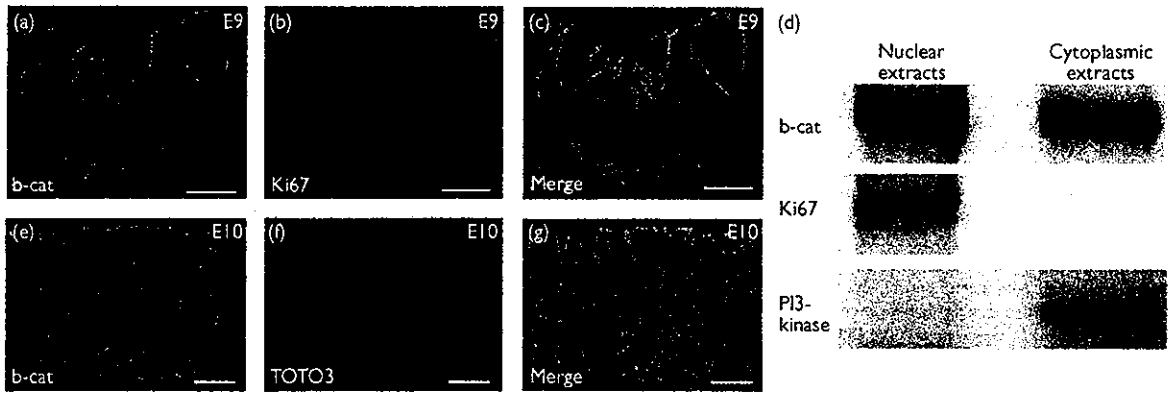

Fig. 1. Localization of β-catenin in developing auditory epithelia on E9 and E10. Immunostaining for β-catenin (b-cat) is found not only at the plasma membrane but also in the nucleus and cytoplasm of epithelial cells on E9 (a–c) and E10 (e–g). Ki67 (b, c) and TOTO3 (f, g) demonstrate nuclear location. Western blotting also demonstrates nuclear and cytoplasmic distribution of β-catenin on E10 (d). Nuclear extracts exhibit expression of Ki67, while cytoplasmic extracts exhibit expression of phosphatidylinositol 3-kinase (PI3-kinase). Scale bars=10 μm.

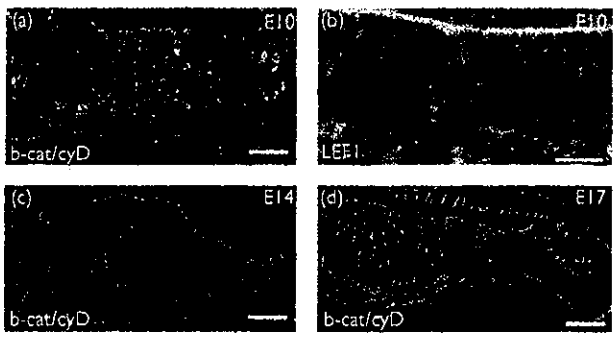

Fig. 2. Expression of β-catenin, lymphoid enhancer factor (LEF) 1 and cyclin D in developing auditory epithelia. Immunostaining for β-catenin (b-cat: green) and cyclin D (cyD: red) represented in a, c and d. On E10, numerous epithelial cells exhibited expression of cyclin D (cyD: red in a), LEF1 (b) and nuclear or cytoplasmic distribution of β-catenin and cytoplasmic membranes (b-cat: green in a). On E14 (c) and E17 (d), the cells expressing cyclin D obviously decrease, and expression of β-catenin is found at the cytoplasmic membrane. Scale bars=20 μm.

Particular attention has been paid to Wnt signalling because of its importance in cell proliferation, fate specification, migration and polarity [18]. Involvement of Wnt proteins or genes in inner ear morphogenesis has also been demonstrated in chicks [19], rats [20] and mice [21]. In mice, expression of Wnt proteins or genes in the auditory epithelium has been observed after E14. However, in the present study, activation of β-catenin signalling in auditory epithelia was observed before E14, suggesting that Wnt signalling may not be involved in activation of β-catenin signalling in auditory epithelia observed in the present study. Wnt-independent pathways, for instance the integrin-linked kinase-mediated pathway, can induce accumulation of β-catenin [22]. In addition, several growth factors also cause accumulation of β-catenin in the cytoplasm by tyrosine phosphorylation of β-catenin that disrupts binding of β-catenin to cadherin [23]. Further investigations are necessary to clarify signalling pathways for accumulation of β-catenin in developing auditory epithelia.

In contrast to the present study, the nuclear translocation of β-catenin in developing auditory epithelia has not been identified in previous studies [9,11]. In these studies, primary antibodies against amino acids 571–781 of β-catenin were used, while the present study used a primary antibody against amino acids 681–781 of β-catenin. The binding of β-catenin to E-cadherin is regulated by the status of β-catenin Tyr654 [23]. Phosphorylation of β-catenin Tyr654 induces the release of β-catenin from E-cadherin. Therefore, Tyr654 of β-catenin located in the cytoplasm or nucleus may be phosphorylated, which can affect the reactivity of the antibody against the 571–781 amino acids of β-catenin. The difference in antibodies used may therefore cause the discrepancy in cellular distribution of β-catenin in auditory epithelia between the previous and present results.

CONCLUSION

The present findings demonstrate that nuclear translocation of β-catenin occurred in cells in developing auditory epithelia together with expression of LEF1 at the same time that active cell proliferation occurs in this system. These findings indicate that β-catenin plays certain roles in cell proliferation during morphogenesis of the developing auditory system.

REFERENCES

1. Nagafuchi A, Takeichi M. Transmembrane control of cadherin-mediated cell adhesion: a 94 kDa protein functionally associated with a specific region of the cytoplasmic domain of E-cadherin. *Cell Regul* 1989; 1:37–44.
2. Cadigan KM, Nusse R. Wnt signaling: a common theme in animal development. *Genes Dev* 1997; 11:3286–3305.
3. Chenn A, Walsh CA. Increased neuronal production, enlarged forebrains and cytoarchitectural distortions in beta-catenin overexpressing transgenic mice. *Cereb Cortex* 2003; 13:599–606.
4. de Melker AA, Desban N, Duband JL. Cellular localization and signaling activity of beta-catenin in migrating neural crest cells. *Dev Dyn* 2004; 230:708–726.
5. Hirabayashi Y, Itoh Y, Tabata H, Nakajima K, Akiyama T, Masuyama N *et al.* The Wnt/beta-catenin pathway directs neuronal differentiation of cortical neural precursor cells. *Development* 2004; 131:2791–2801.
6. Morsli H, Choo D, Ryan A, Johnson R, Wu DK. Development of the mouse inner ear and origin of its sensory organs. *J Neurosci* 1998; 18:3327–3335.

7. Leonova EV, Raphael Y. Organization of cell junctions and cytoskeleton in the reticular lamina in normal and ototoxically damaged organ of Corti. *Hear Res* 1997; 113:14–28.
8. Whitlon DS, Zhang X, Pecelunas K, Greiner MA. A temporospatial map of adhesive molecules in the organ of Corti of the mouse cochlea. *J Neurocytol* 1999; 28:955–968.
9. Matsuda M, Keino H. Roles of beta-catenin in inner ear development in rat embryos. *Anat Embryol (Berl)* 2000; 202:39–48.
10. Kim TS, Nakagawa T, Endo T, Iguchi F, Murai N, Naito Y *et al.* Alteration of E-cadherin and beta-catenin in mouse vestibular epithelia during induction of apoptosis. *Neurosci Lett* 2002; 329:173–176.
11. Simonneau L, Gallego M, Pujol R. Comparative expression patterns of T-, N-, E-cadherins, beta-catenin, and polysialic acid neural cell adhesion molecule in rat cochlea during development: implications for the nature of Kolliker's organ. *J Comp Neurol* 2003; 459:113–126.
12. Tetsu O, McCormick F. Beta-catenin regulates expression of cyclin D1 in colon carcinoma cells. *Nature* 1999; 398:422–426.
13. Nelson WJ, Nusse R. Convergence of Wnt, beta-catenin, and cadherin pathways. *Science* 2004; 303:1483–1487.
14. Roberson DW, Rubel EW. Cell division in the gerbil cochlea after acoustic trauma. *Am J Otol* 1994; 15:28–34.
15. Huber O, Korn R, McLaughlin J, Ohsugi M, Herrmann BG, Kemler R. Nuclear localization of beta-catenin by interaction with transcription factor LEF-1. *Mech Dev* 1996; 59:3–10.
16. Behrens J, von Kries JP, Kuhl M, Bruhn L, Wedlich D, Grosschedl R *et al.* Functional interaction of beta-catenin with the transcription factor LEF-1. *Nature* 1996; 382:638–642.
17. Shtutman M, Zhurinsky J, Simcha I, Albanese C, D'Amico M, Pestell R *et al.* The cyclin D1 gene is a target of the beta-catenin/LEF-1 pathway. *Proc Natl Acad Sci USA* 1999; 96:5522–5527.
18. Huelsken J, Birchmeier W. New aspects of Wnt signaling pathways in higher vertebrates. *Curr Opin Genet Dev* 2001; 11:547–553.
19. Stevens CB, Davies AL, Battista S, Lewis JH, Fekete DM. Forced activation of Wnt signaling alters morphogenesis and sensory organ identity in the chicken inner ear. *Dev Biol* 2003; 261:149–164.
20. Daudet N, Ripoll C, Moles JP, Rebillard G. Expression of members of Wnt and frizzled gene families in the postnatal rat cochlea. *Brain Res Mol Brain Res* 2002; 105:98–107.
21. Dabdoub A, Donohue MJ, Brennan A, Wolf V, Montcouquiol M, Sassoon DA *et al.* Wnt signaling mediates reorientation of outer hair cell stereociliary bundles in the mammalian cochlea. *Development* 2003; 130:2375–2384.
22. Novak A, Hsu SC, Leung-Hagesteijn C, Radeva G, Papkoff J, Montesano R *et al.* Cell adhesion and the integrin-linked kinase regulate the LEF-1 and beta-catenin signaling pathways. *Proc Natl Acad Sci USA* 1998; 95:4374–4379.
23. Roura S, Miravet S, Piedra J, Garcia de Herreros A, Dunach M. Regulation of E-cadherin/catenin association by tyrosine phosphorylation. *J Biol Chem* 1999; 274:36734–36740.

Acknowledgements: This study was supported by a Grant-in-Aid for Scientific Research (14207068), a Grant-in-Aid for Exploratory Research (15659405), a Grant-in-Aid for Regenerative Medicine Realization Project and Establishment of International COE for Integration of Transplantation Therapy and Regenerative Medicine (COE program) from the Ministry of Education, Science, Sports, Culture and Technology of Japan. We thank Professor Edwin W. Rubel (Department of Otolaryngology, University of Washington, Seattle, Washington, USA) for his valuable comments.

Cell Therapy for Inner Ear Diseases

T. Nakagawa* and J. Ito

Department of Otolaryngology-Head and Neck Surgery, Kyoto University Graduate School of Medicine, Kyoto, Japan

Abstract: Degeneration of inner ear cells, especially sensory hair cells and associated neurons, results in hearing impairment and balance disorders. These disabilities are incurable because loss of hair cells and associated neurons is currently irreversible. Protection or regeneration of hair cells and associated neurons is an important area of research for developing an effective treatment for inner ear diseases. Cell therapy is a rapidly growing area of research and has potential applications in the treatment of inner ear disorders. The first attempts to examine the feasibility of cell therapy in the treatment of inner ear disorders have been performed using neural stem cells (NSCs). Grafted NSCs can survive in the inner ear and differentiate into neural, glial and/or hair cell-phenotypes, making NSC transplantation for the restoration of inner ear cells a potentially viable treatment. Further studies have suggested embryonic stem cells (ESCs), dorsal ganglion cells and cell lines derived from fetal inner ear cells could be used to restore damaged inner ear cells. Cell transplantation has also been suggested as a strategy for drug delivery into the inner ear, and the ability of NSC-derived cells to produce neurotrophins in the inner ear has been demonstrated. Results from studies using autologous bone marrow stromal cells (MSCs) indicate a high survival and migration potential suggesting that MSCs can be used as a drug delivery vehicle to the inner ear. These cell transplantation findings provide a sound foundation for the development of therapies to treat inner ear disorders.

Key Words: Cell transplantation, inner ear, regeneration, protection, drug delivery.

BACKGROUND

Hearing impairment is one of the most common disabilities in industrialized countries. Hearing depends largely on hair cells and their associated spiral ganglion neurons and defects in these cells result in hearing loss or deafness. In addition, the vestibular sensory epithelia are also located in the inner ear and suffer progressive losses. Loss of mammalian auditory hair cells is currently irreversible [1, 2]. Regeneration of vestibular hair cells in adult mammals is very limited [3-6], although the potential to produce new hair cells has been investigated [5, 7, 8]. In fact, there are currently no clinical treatments available for the loss of vestibular hair cells. Loss of auditory function due to degeneration of auditory hair cells can be partly restored by cochlear implants, which are small devices surgically implanted in the inner ear to stimulate the spiral ganglion neurons. However, the cochlear implant depends on remaining spiral ganglion neurons, and their loss severely compromises its efficacy. If regeneration of hair cells and spiral ganglion neurons were possible, then impaired inner ear function might be restored; however, functional recovery by regeneration of hair cells or spiral ganglion neurons is currently impossible.

Many attempts have been made to elucidate the progenitor cell for newly produced hair cells and mechanisms for stimulating its division and differentiation, or transdifferentiation. Studies have shown that some molecules can stimulate proliferation of supporting cells (candidates of progenitors) [9-11] and induce phenotypic conversion of these cells [12-14]. One potential method for the replacement of lost cells involves the delivery of these molecules to supporting cells. Some *in vitro* studies have shown that treating supporting cells with growth factors and cAMP induces proliferation [11, 15]; however, promotion of cell proliferation in sensory epithelia of the mammalian inner ear by growth factors has not been demonstrated *in vivo*. Gene transfer provides a potentially powerful method of introducing these molecules into the inner ear [16-18]. Strikingly, it has been demonstrated that overexpression of Math 1, which is a molecule regulating the Notch signaling pathway, induces the appearance of newly produced hair cells in mammalian auditory epithelia *in vivo* [19]. Gene transfer into inner ear cells may become a feasible therapy when the gene vehicles improve.

Protecting hair cells and associated neurons from irreversible degeneration has been a primary objective because inner ear cells have limited regeneration activity. Efforts to reduce degeneration of hair cells and associated neurons identified several agents for protection of hair cells and/or spiral ganglion neurons. Experimentally, protective effects of neurotrophins have been demonstrated [20, 21], and inhibitors of apoptosis and glutamate antagonists have also shown the ability to promote hair cell survival [22-24]. These agents were applied directly to the inner ear, and not administered systemically. One reason for direct delivery of the agent is the existence of the blood-inner ear barrier, which blocks transport of agents from the blood to the inner ear. Another reason is that some of these agents cannot be administered systemically because of their side effects. Therefore, developing strategies for local delivery into the inner ear is crucial for developing clinical therapies based on the experimental findings. In previous investigations, micro-

*Address correspondence to this author at the Department of Otolaryngology-Head and Neck Surgery, Kyoto University Graduate School of Medicine, 54 Kawahara-cho, Shogoin, Sakyo-ku, 606-8507 Kyoto, Japan; Tel: +81-75-751-3346, Fax: +81-75-751-7225,
E-mail: tnakagawa@ent.kuhp.kyoto-u.ac.jp

1381-6128/05 $50.00+.00

infusion pumps and gene transfer using virus vectors were used as strategies for drug delivery [16, 21]. Another route is *via* diffusion across the round window [25]. These methods have been proven to be effective for protection of inner ear cells from degeneration.

Cell therapy may be an effective way of replacing or protecting hair cells and associated neurons in the inner ear, and cell transplantation has received attention as a novel strategy for repairing the nervous system by actually restoring lost cells. In the central nervous system, restoration of neurons by transplantation of neural stem cells (NSCs) or embryonic stem cell (ESC)-derived cells has been demonstrated [26, 27]. Functional recovery of an injured spinal cord following NSC transplantation has been seen in animal models [28]. A great deal of progress has also been achieved in the visual system, where retinal transplantation of NSCs or ESC-derived cells can restore retinal cells [29, 30]. In addition, sensory recovery of the retina has also been measured in the superior colliculus [31]. Furthermore, clinical application of angiogenesis by cell transplantation has begun [32, 33]. These advances in stem cell biology have encouraged investigation into the potential of cell transplantation for restoring hair cells and associated neurons in the inner ear. Cell therapy could potentially enable long-term delivery of several agents into the inner ear, and cell transplantation has been used as means to deliver peptides or proteins into the central nervous system [34-37] demonstrating that transplanted cells can be used as a vehicle for drug or gene delivery.

HAIR CELL REGENERATION

Sensory hair cells in the inner ear adapt mechanical stimulation and convert mechanical stimulation into electric signals. Sensory hair cells are therefore crucial for sound adaptation, and have been considered as primary sites for inner ear diseases. To effect cell transplantation for hair cell regeneration, transplantation of NSCs into the cochlea of newborn rats has been attempted [38], because the potential of NSCs for restoration of retinal cells has been indicated [29]. NSCs can survive in the inner ear and the incorporation of some grafted NSCs in auditory epithelia of newborn rats as well as in the retina. In addition, the survival of NSC-derived cells after transplantation into the mature inner ear of mice has been demonstrated [39]. However, no or few NSC-derived cells have found in sensory epithelia of the inner ear. Then, the activity of NSCs for migration into sensory epithelia damaged by ototoxic agents was investigated, because the considerable activity of NSCs for migration into the retina after traumatic injury has been reported [29]. Surprisingly, some NSC-derived cells settled in vestibular epithelia exhibit a hair cell-specific marker indicating NSCs possess the ability to differentiate into hair cells *in vivo* [40]. Similar findings to show the potential of NSCs for transdifferentiation into hair cells have been reported from the other laboratory [41]. *In vitro* investigations, which demonstrate that neurospheres derived from embryonic rat brain give rise to hair cell phenotypes [42], support the hypothesis that NSCs can be a source for regenerating hair cells. These findings indicate that cell transplantation is a possible strategy for hair cell regeneration, although functional recovery by NSC transplantation has not been demonstrated.

ESCs could potentially be used for hair cell regeneration because of the pulripotent. Undifferentiated ESCs grafted into the inner ear, however, have no potential to differentiate into hair cell phenotypes [43], indicating that the damaged or immature inner ear does not have enough activity to induce differentiation of ESCs into hair cells. On the other hand, the potential of ESCs for differentiation into a hair cell-phenotype has been demonstrated following stepwise induction [44], which suggests that ESCs can be a source for regenerating hair cells following appropriate manipulation.

An alternative is cell lines originating from inner ear tissues. Several cell lines derived from developing inner ear epithelia have been established but most lines are derived from a transgenic animal that carries a conditionally expressed immortalizing gene [45, 46]. However, cell lines from otocysts of wild type rats have been established by a combination of limited dilution and retroviral gene-marking methods [47]. Otocyst-derived cells express immature cell features for up to 6 months in cell culture. Cells from a one-week-old culture provided with a high seeding density and supplemented with epidermal growth factor can be differentiated into phenotypes of hair cells, supporting cells or neurons. In addition, these cells have migration activity into auditory epithelia *in vivo* [48]. These findings suggest that the cells obtained from embryonic inner ear epithelia may be desirable restoration transplants for hair cells, although their availability has remained an unsolved problem. Recent studies have indicated that stem or progenitor cells for inner ears are available from auditory [49] or vestibular sensory epithelia [50] of adult mammals. Therefore, there is a possibility that stem or progenitor cells for inner ears are obtained from surgical specimens.

REGENERATION OF SPIRAL GANGLION NEURONS

The first animal experiments on the auditory system to examine the potential for repair of the central auditory pathway have been performed [51]. Embryonic brain tissue was transplanted into a lesion in the ventral cochlear tract resulting in tissue regeneration and associated functional recovery. These findings suggest that cell therapy can be used for the treatment of auditory nervous systems. NSCs are included in candidates of transplants for regeneration of auditory nervous systems. NSCs grafted into the cochlea fluid space differentiate into neural or glial cells [39, 40], indicating the potential use of NSC transplantation for restoration of spiral ganglion neurons. Then, the ability of NSCs to undergo neural differentiation in the cochlear modiolus, which contains spiral ganglion neurons and auditory nerve fibers, was investigated [52]. Grafted NSCs can survive and differentiate into neurons in the cochlear modiolus, suggesting the possible use of NSCs, in cell therapy, to restore spiral ganglion neurons. Another candidate for neuronal transplants is dorsal root ganglion cells (DRGs). A series of studies using fetal DRGs has shown their potential as transplants for restoration of spiral ganglion neurons [53, 54, 55]. DRGs grafted into the cochlea fluid space can survive in the cochlea, and a part of grafted